The hVPS34-SGK3 signalling module counteracts inhibition of the PI3K-Akt pathway to stimulate mTORC1 and tumour growth

Ruzica Bago[1], Eeva Sommer[1], Pau Castel[2], Claire Crafter[3], Fiona P. Bailey[4], Natalia Shpiro[1], José Baselga[2], Darren Cross[3], Patrick A. Eyers[4] and Dario R. Alessi[1]

1. MRC Protein Phosphorylation and Ubiquitylation Unit, College of Life Sciences, University of Dundee, Dundee DD1 5EH

2. Human Oncology and Pathogenesis Program and Memorial Sloan Kettering Cancer Center, 1275 York Avenue, Box 20, New York, NY 10065, USA.

3. Oncology iMED, AstraZeneca, CRUK Cambridge Institute, Cambridge, CB2 0RE , UK

4. Department of Biochemistry, Institute of Integrative Biology, University of Liverpool, Liverpool, L69 7ZB

Correspondence to RB (r.bago@dundee.ac.uk) or DRA (d.r.alessi@dundee.ac.uk)

Key Words
Protein kinase inhibitors; signal transduction inhibitors; PI3K and NDRG1, SGK3, NanoString, mTORC1, mTORC2

Abbreviations
mTOR (mammalian target of rapamycin), NDRG1 (N-myc downstream-regulated gene-1), PC (phosphatidylcholine), PS (phosphatidylserine), PtdIns (phosphatidylinositol), PtdIns(3)P (phosphatidylinositol-3-phosphate), PDK1 (Phosphoinositide-Dependent Kinase-1), PI3K (Phosphoinositide 3-kinase), PH (pleckstrin homology), PRAS40 (proline-rich Akt substrate 40 kDa), PX (phox homology), SGK3 (serum and glucocorticoid regulated kinase-3), hVps34 (human Vacuolar protein sorting 34)

Abstract
We explore mechanisms that enable cancer cells to tolerate PI3K or Akt inhibitors. Prolonged treatment of breast cancer cells with PI3K or Akt inhibitors leads to increased expression and activation of a kinase termed SGK3 that is related to Akt. Under these conditions, SGK3 is controlled by hVps34 that generates PtdIns(3)P, which binds to the PX domain of SGK3 promoting phosphorylation and activation by its upstream PDK1 activator. Furthermore, under conditions of prolonged PI3K/Akt pathway inhibition, SGK3 substitutes for Akt by phosphorylating TSC2 to activate mTORC1. We characterise 14h, a compound that inhibits both SGK3 activity and activation in vivo and show that a combination of Akt and SGK inhibitors induced marked regression of BT-474 breast cancer cell derived tumours in a xenograft model. Finally, we present the kinome-wide analysis of mRNA expression dynamics induced by PI3K-Akt inhibition. Our findings highlight the importance of the hVps34-SGK3 pathway and suggest it represents a mechanism to counteract inhibition of PI3K/Akt signalling. The data support the potential of targeting both Akt and SGK as a cancer therapeutic.

Introduction

The majority of human tumours harbour mutations promoting inappropriate activation of the Akt kinase and therefore inhibitors of Akt and its upstream activators including Class I PI3K are being evaluated in many cancer clinical trials (Bauer et al, 2015; Liu et al, 2009; Vanhaesebroeck et al, 2012). Despite the benefit observed with these molecules, drug resistance can emerge as a result of adaptive mechanisms limiting the use of these therapies (Rodon et al, 2013). Therefore, understanding and reverting mechanisms of resistance to PI3K/Akt inhibitors is expected to improve the success of the treatment.

The Class I PI3K family (p110α, p110β, p110γ and p110δ), is activated in response to extracellular stimuli and phosphorylates the 3'-hydroxyl group of the inositol moiety of membrane bound phosphatidylinositol 4,5 bisphosphate (PtdIns (4,5)P_2) to generate PtdIns(3,4,5)P_3 (Cantley, 2002; Vanhaesebroeck et al, 2001). PtdIns(3,4,5)P_3 and its immediate breakdown product PtdIns(3,4)P_2, recruit Akt and its upstream regulator phosphoinositide-dependent kinase 1 (PDK1) to the plasma membrane via their PtdIns(3,4,5)P_3/PtdIns(3,4)P_2-binding PH domains (Mora et al, 2004). This induces a conformational change in Akt enabling PDK1 to phosphorylate its T-loop Thr308 residue (Alessi et al, 1997a; Alessi et al, 1997b; Stephens et al, 1998; Stokoe et al, 1997). Akt is fully activated following phosphorylation by mTORC2 (mammalian target of rapamycin complex-2) at the hydrophobic motif Ser473 residue that lies within the C-terminal non-catalytic region (Sarbassov et al, 2005). Ser473 phosphorylation also promotes interaction of Akt with PDK1 enhancing phosphorylation of Thr308 (Najafov et al, 2012). A recent study has suggested that PtdIns(3,4,5)P_3 stimulates Ser473 phosphorylation by binding to the PH domain of the mTORC2 complex Sin1 subunit (Liu et al, 2015).

Although the focus has been on the role that Akt isoforms play in mediating proliferation responses that are controlled by Class I PI3Ks, increasing evidence is accumulating that isoforms of serum and glucocorticoid regulated kinases (SGK) which share ~50% identity within their catalytic domains to Akt, also control proliferation and survival responses in cancer cells (Bago et al, 2014; Bruhn et al, 2010; Bruhn et al, 2013; Gasser et al, 2014; Pearce et al, 2010; Vasudevan et al, 2009). Although SGK1 and SGK2 isoforms lack a PH domain they are still activated by Class I PI3Ks (Kobayashi & Cohen, 1999; Kobayashi et al, 1999) through their ability to induce hydrophobic motif phosphorylation via mTORC2, which in turn triggers phosphorylation of the T-loop residue by PDK1 (Biondi et al, 2001; Collins et al, 2003; Collins et al, 2005). SGK and Akt kinases possess similar substrate specificities with both enzymes preferring to phosphorylate Ser/Thr residues lying within Arg-Xaa-Arg-Xaa-Xaa-Ser/Thr (where Xaa is any amino acid) motifs (Alessi et al, 1996; Murray et al, 2005). Consistent with this, several Akt substrates including FOXO transcription factors (Brunet et al, 2001), GSK3 (Dai et al, 2002; Kobayashi & Cohen, 1999) and NDRG1 (Sommer et al, 2013) are similarly phosphorylated by SGK1. It is therefore likely that in tumours displaying activated PI3K signalling, both Akt1/2 and SGK1/SGK2 would be elevated and stimulate proliferation by phosphorylating an overlapping subset of substrates. The sensitivity of a group of breast cancer cell lines possessing mutations that activate the PI3K pathway to

Akt inhibitors has been correlated with the expression of SGK1 in cell lines including ZR-75-1, CAMA-1 and T47D (utilised in this study). Interestingly, these lines all contain low endogenous SGK1 levels and are intrinsically more sensitive to Akt inhibitors than cells that express higher levels of SGK1 (Sommer et al, 2013).

In contrast to other SGK isoforms, SGK3 possesses an N-terminal PtdIns(3)P binding PX domain (Bago et al, 2014; Virbasius et al, 2001) and is the only known kinase to possess a PtdIns(3)P interaction domain (Pearce et al, 2010). SGK3 associates with endosome membranes, where the Class III PI3K family member termed hVps34 phosphorylates PtdIns to generate a large fraction of the cellular pool of PtdIns(3)P (Backer, 2008; Bago et al, 2014; Gillooly et al, 2000). Mutations within the SGK3 PX domain that ablate PtdIns(3)P binding or treatment of cells with a hVps34 inhibitor to reduce PtdIns(3)P levels, blocked SGK3 endosomal localisation and also suppressed SGK3 activity, by lowering phosphorylation of T-loop and hydrophobic motifs (Bago et al, 2014).

In the present study we demonstrate that prolonged treatment of several breast cancer cell lines (ZR-75-1, CAMA-1, T47D and BT-474c) harbouring mutations that activate the Akt signalling pathway with inhibitors of Class I PI3K or Akt, lead to marked upregulation of SGK3 mRNA, and subsequent activation of the SGK3 protein kinase. Employing structurally diverse specific hVps34 inhibitors (VPS34-IN1 and SAR405), we establish that SGK3 activation induced by prolonged treatment with Class I PI3K or Akt inhibitors is controlled by hVps34. Mechanistic studies reveal that PtdIns(3)P binding to the PX domain of SGK3, promotes phosphorylation and activation by its upstream PDK1 activator. Moreover, we show that following prolonged inhibition of the PI3K-Akt pathway, SGK3 could substitute for Akt and promote activation of mTORC1 and hence S6K1 by phosphorylating TSC2 at the same sites as Akt. We discover that a previously reported SGK1 inhibitor termed 14h (Halland et al, 2015), also potently inhibits SGK3 (IC50 of 4 nM) with 2.5-fold higher potency than SGK1 and in addition blocks SGK3 activation by PDK1 and mTORC2 in cells. Moreover, we show that a combination of Akt (MK-2206) and SGK (14h) inhibitors induces marked regression of tumour volume in a nude mouse xenograft model derived from BT-474 breast cancer cells. Finally, we present a kinome-wide analysis of mRNA expression dynamics induced in response to PI3K-Akt pathway inhibition. Our findings highlight the importance of the hVps34-SGK3 pathway, which is likely to represent a major mechanism that can be used by cells to counteract inhibition of the PI3K-Akt signalling network. Our results clearly emphasise the therapeutic potential of targeting both the Akt and SGK kinases for the treatment of cancer.

RESULTS

Prolonged treatment with Akt and Class I PI3K inhibitors leads to upregulation of SGK3. Treatment of breast cancer cell lines ZR-75-1 and CAMA-1 that have low levels of SGK1 (Sommer et al, 2013) with structurally diverse Akt inhibitors (MK-2206 (Hirai et al, 2010) and AZD5363 (Davies et al, 2012)) for 1 hour, inhibited phosphorylation of PRAS40 (Thr246, Akt specific substrate) as well as NDRG1 (Thr346, Akt and SGK substrate) (Fig 1A). MK-2206 is an allosteric inhibitor that suppresses Thr308 and Ser473 phosphorylation (Hirai et al, 2010), whereas AZD5363 is a catalytic inhibitor that despite ablating Akt activity in cells leads to increased phosphorylation of Thr308 and Ser473 by modulating feedback loops (Davies et al, 2012). Strikingly however, prolonged Akt inhibitor treatment over 1-10 days, led to a time-dependent recovery of NDRG1 phosphorylation, under conditions where the Akt substrate PRAS40 remained dephosphorylated (Fig 1A). Immunoblotting revealed that prolonged Akt inhibitor treatment enhanced expression of SGK3 protein over this period under conditions where SGK1 remained undetectable (Fig 1A). Quantitative mRNA analysis by RT-PCR revealed that Akt inhibitors induced 3 to 6-fold increase in SGK3 mRNA levels after 2 to 10 days, whereas SGK1 or SGK2 mRNA levels were unaltered (Fig 1B). Interestingly, knock-down of SGK3 protein expression employing 3 distinct shRNA probes, blocked prolonged Akt inhibitor treatment from enhancing NDRG1 phosphorylation in both ZR-75-1 and CAMA-1 cells (Fig 1C).

Similarly, treatment of ZR-75-1, CAMA-1, and T47D cultured in serum with structurally diverse Class I PI3K inhibitors GDC0941 (Folkes et al, 2008) and BKM120 (Bendell et al, 2012) for 1 hour also markedly suppressed NDRG1 and PRAS40 phosphorylation (Fig 2A). Analogous to what was observed with prolonged Akt inhibitor treatment (Fig 2A), prolonged treatment with Class I PI3K inhibitors induced up-regulation of SGK3 mRNA and protein levels that was accompanied by an increase in NDRG1 phosphorylation (Fig 2A and SFig1). The induction of SGK3 protein and mRNA levels was more pronounced in ZR-75-1 or CAMA-1 cells than T47D cells, but nevertheless in all 3 cell lines, prolonged treatment with Class I PI3K or Akt inhibitors induced a similar significant increase in NDRG1 phosphorylation.

Prolonged treatment with Class I PI3K and Akt inhibitors leads to activation of SGK3. To study the effect that Class I PI3K (GDC0941 and BKM120) and Akt inhibitors (MK-2206 and AZD5363) had on SGK3 kinase activity, we immunoprecipitated endogenous SGK3 and assessed protein kinase activity by measuring phosphorylation of the Crosstide substrate peptide (Bago et al, 2014). In all cell lines tested (ZR-75-1, CAMA1 and T47D) short term treatment (1hour) with Akt and Class I PI3K inhibitors induced transient reduction in SGK3 activity without affecting SGK3 protein levels. The underlying mechanism behind this is not clear. In both ZR-75-1 and CAMA-1 cells, prolonged treatment (5 days) with Class I PI3K or Akt inhibitors induced a robust 2 to 4-fold increase in SGK3 protein kinase activity (Fig 2B). More moderate increases SGK3 phosphorylation and activity was observed in T47D cells, consistent with the lower induction of SGK3 (Fig 2A). Immunoblot analysis of SGK3

immunoprecipitates confirmed that prolonged treatment with Class I PI3K or Akt inhibitors increased SGK3 protein as well as T-loop and hydrophobic motif phosphorylation (Fig 2B).

Class III PI3K, hVps34, controls SGK3 activity. To explore the role that hVps34 might play in regulating endogenous activity of SGK3 induced by prolonged treatment with Akt inhibitors, we treated ZR-75-1 cells for 5 days with MK-2206 and then incubated cells for one hour with increasing doses of highly selective and structurally diverse hVps34 inhibitors, namely VPS34-IN1 (Bago et al, 2014) or SAR405 (Ronan et al, 2014). In ZR-75-1 cells pre-treated with Akt inhibitor (MK-2206) for 5 days, both inhibitors induced a dose dependent inhibition of NDRG1 phosphorylation with VPS34-IN1 reducing NDRG1 phosphorylation to basal levels at 1 μM (Fig 3A) and SAR405 at 0.3 μM (SFig 2A), consistent with the higher potency of SAR405 inhibitor towards hVps34 (Bago et al, 2014; Ronan et al, 2014). In agreement with VPS34-IN1 or SAR405 having no inhibitory activity towards Class I PI3K, neither compound suppressed Akt phosphorylation or PRAS40 phosphorylation (Fig 3B & SFig 2B). Elevated SGK3 protein kinase activity as well as T-loop and hydrophobic motif phosphorylation induced by prolonged treatment with Class I PI3K or Akt inhibitors, was also suppressed by treatment with 1 μM VPS34-IN1 (Fig 3C) or 0.3 μM SAR405 (SFig 2C). Treatment of ZR-75-1 cells cultured in serum for 1 hour with 1 μM VPS34-IN1 (Fig 3C) or 0.3 μM SAR405 (SFig 2C) also reduced the basal SGK3 activity and phosphorylation detected in these cells to below control levels.

mTORC2 regulates activation of SGK3 downstream of hVPS34. The identity of the hydrophobic motif kinase that phosphorylates SGK3 downstream of hVps34 has not been established. Since mTORC2 regulates activation of SGK1 (Garcia-Martinez & Alessi, 2008), we wished to explore whether mTORC2 also mediates SGK3 hydrophobic motif phosphorylation under conditions of prolonged treatment with Class I PI3K or Akt inhibitors. To achieve this, we generated ZR-75-1 cells in which the Rictor subunit of mTORC2 (Sarbassov et al, 2005), was knock-down by ~90% employing an shRNA approach (Fig 3D). Consistent with efficient knock-down of Rictor and suppression of mTORC2 activity, Akt Ser473 phosphorylation was markedly reduced in the Rictor shRNA knock-down cells whereas phosphorylation of S6 protein, which is controlled in a Rictor independent manner by mTORC1 was unaffected (Fig 3D). Knock-down of Rictor also virtually ablated kinase activity as well as the hydrophobic motif phosphorylation of SGK3 induced by prolonged treatment with Class I or Akt kinase inhibitors (Fig 3D). Treatment of ZR-75-1 cells with the mTOR catalytic inhibitor AZD8055 that inhibits both mTORC1 and mTORC2 suppressed SGK3 hydrophobic motif and T-loop phosphorylation as well as SGK3 kinase activity (Fig 3E). However, mTORC1 specific inhibitor rapamycin that does not inhibit mTORC2 at this concentration, had no effect on SGK3 phosphorylation or activity (Fig 3E).

PtdIns(3)P promotes phosphorylation and activation of SGK3 by PDK1. To investigate whether PtdIns(3)P that is produced by hVps34 could promote phosphorylation and activation of SGK3, we utilised recombinant SGK3[S486E], in which the hydrophobic motif was mutated to Glu to mimic mTORC2

phosphorylation and promote phosphorylation by PDK1 (Biondi et al, 2001). SGK3[S486E] was purified from HEK293 cells that had been treated with hVps34 (VPS34-IN1, 5 μM) and PDK1 inhibitor (GSK2334470, 5 μM) (Najafov et al, 2011) for 1 hour, to ensure that SGK3 was in its dephosphorylated and inactive form. SGK3[S486E] purified in this manner was incubated with lipid vesicles comprising phosphatidylcholine (PC) and phosphatidylserine (PS) containing either increasing concentrations of PtdIns(3)P or PtdIns. Kinase reactions were initiated by addition of PDK1 and MgATP. Activation of SGK3[S486E] was assessed by monitoring phosphorylation of SGK3 at Thr320 (PDK1 site) and as well as NDRG1 at Thr346 (SGK1 site). These studies revealed that activation of SGK3[S486E] beyond background levels was only observed in the presence of PS/PS vesicles containing PtdIns(3)P (Fig 4A). Even at the highest concentration of PtdIns tested (10 μM), no significant activation of SGK3[S486E] beyond control levels was observed. We found that SGK3[S486E] isolated from HEK293 cells was contaminated with endogenous PDK1 (FIG 4-see high exposure immunoblot), which is consistent with the ability of SGK3[S486E] to bind PDK1 with high affinity (Biondi et al, 2001). Therefore, even in the absence of added recombinant PDK1, incubation of SGK3[S486E] with PC/PS vesicles containing PtdIns(3)P and MgATP lead to partial activation, under conditions where no detectable activation is observed when PtdIns(3)P is replaced with PtdIns (Fig 4B). Addition of 50 ng recombinant PDK1 led to further activation of SGK3[S486E] in the presence of PtdIns(3)P but not PtdIns (Fig 4B). Mutation of PX domain residue Arg90, required for interaction of SGK3 with PtdIns(3)P (Bago et al, 2014), prevented activation of SGK3[S486E] by PDK1 in the presence of PtdIns(3)P (Fig 4B).

14h is a potent inhibitor of SGK3. Recently, Sanofi published a new series of SGK1 inhibitors (Halland et al, 2015). As the potency of these compounds towards the SGK3 isoform was not reported, we synthesized and evaluated the selectivity of the four most potent SGK1 inhibitors (14g, 14h, 14i and 14n) described in this study (Fig 5A and SFig 3A). We confirmed that these compounds inhibited SGK1 with an IC50 of 10-70 nM and found that these compounds also targeted SGK3 with an IC50 of 4-80 nM (Fig 5B and SFig 3B). The 14h inhibitor was the most potent against SGK3, displaying an IC50 of 4 nM, which is 2.5-fold more potent than it inhibits SGK1 (10 nM) (Fig 5B). The selectivity of these inhibitors was assessed using the Dundee panel of 140 kinases (Fig 5C for 14h and SFig 4 for 14g, 14i and 14n and STable1-4). All four SGK inhibitors displayed similar selectivity with the major off target kinases being S6K1, MLK1, MLK3, and TIE2 (Fig 5C for 14h and SFig 4 for 14g, 14i, and 14n and STable1-4). We observed that the SGK inhibitors (14g, 14h, 14i, and 14n) also supressed S6K1 with IC50 of 55 to 180 nM and MLK isoforms with IC50 of 94 to 600 nM (Fig 5B and SFig 3B). Importantly, none of the SGK inhibitors tested significantly inhibited Akt1, suggesting that these compounds would be useful in discriminating between Akt and SGK mediated responses in vivo (Fig 5B and SFig 3B).

14h suppresses NDRG1 phosphorylation in cells. For cellular experiments we employed 14h, as it was the most potent SGK3 inhibitor (Fig 5B). Treatment of ZR-75-1 cells cultured in serum with increasing doses of 14h for one hour,

resulted in a dose dependent decrease in NDRG1 phosphorylation. NDRG1 phosphorylation was maximally suppressed at 1 to 3 μM 14h, under conditions, where Akt-specific substrate PRAS40 was not dephosphorylated. Consistent with the ~20-fold lower potency of 14h towards S6K1 compared to SGK3 (Fig 5B), 1 to 3 μM 14h failed to significantly inhibit Rictor (Thr1135, S6K1 specific site) and S6 protein (Ser240/244, S6K1 site) phosphorylation (Fig 5D). However at 10 μM 14h, we noticed a moderate reduction in S6K1 and S6 protein phosphorylation (Fig 5D), suggesting that 14h should not be deployed at concentrations of higher than 3 μM in cellular studies.

14h suppresses T-loop and hydrophobic motif phosphorylation of SGK3. Allosteric Akt inhibitors such as MK-2206, in addition to suppressing kinase activity, also inhibit phosphorylation of the T-loop and hydrophobic motifs by trapping Akt in a conformation that cannot be phosphorylated by PDK1 and mTORC2 in cells (Green et al, 2008; Hirai et al, 2010). To determine whether 14h was capable of suppressing SGK3 activation in an analogous manner, we treated ZR-75-1 cells with increasing doses of 14h for one hour and analysed after immunoprecipitation SGK3 the T-loop and hydrophobic motif phosphorylation as well as kinase activity. This revealed that 14h suppressed in a dose dependent manner SGK3 hydrophobic as well as T-loop phosphorylation resulting in reduced SGK3 activity (Fig 5E). At 0.1 μM 14h, SGK3 activity and phosphorylation was reduced by ~80% and undetectable by 1 μM (Fig 5E). In biochemical studies 14h also suppressed the ability of PDK1 to phosphorylate SGK3[S486E] at Thr320 in the presence of PtdIns(3)P, with a near maximal inhibition observed at 0.1 μM 14h (Fig 5F).

SGK3 activates mTORC1 independently of Akt by phosphorylating TSC2. We next treated ZR-75-1 cells with the MK-2206 Akt inhibitor for between 1 hour and 5 days and at intervals measured SGK3 and S6K1 catalytic activity (Fig 6). After 1h treatment with MK-2206 (under conditions where SGK3 activity remains low), ~10-fold reduction of S6K1 activity was observed, which was accompanied by dephosphorylation of Rictor (Thr1135) and S6 protein (Ser240/244) as well as 4EBP1 (Ser65), another key substrate of mTORC1 (Fig 6). This result is consistent with previous work showing that a major substrate of Akt phosphorylation in cancer cells is the tuberous sclerosis complex protein TSC2 (Manning et al, 2002; Menon et al, 2014), which subsequently inhibits GTPase activating protein activity of TSC2, leading to the activation of the Rheb GTPase and hence mTORC1 (Manning et al, 2002; Menon et al, 2014). Consistent with this, 1h treatment with MK-2206 induced dephosphorylation of TSC2 (Ser939, Thr1462) at the sites phosphorylated by Akt. However, after 1-2 days of MK-2206 treatment, as SGK3 is specifically becoming upregulated, we observed a commensurate increase of S6K1 activity that correlates with increased phosphorylation of TSC2 at the Akt sites as well as Rictor, S6 protein and 4EBP1 phosphorylation, under conditions which Akt remains inactivated (Fig 6). After 4 to 5 days MK-2206 treatment, S6K1 activity as well as the phosphorylation of TSC2, Rictor, S6 protein and 4EBP1 had recovered to the similar level that was observed in non-Akt inhibitor treated cells (Fig 6).

As Akt and SGK isoforms have very similar substrate specificity (Murray et al, 2005), our data indicate that SGK3 might functionally substitute for Akt in phosphorylating TSC2 in cells lacking Akt activity. To investigate this further, we treated ZR-75-1 cells for 5 days with either Class I PI3K (GDC0941) or Akt (MK-2206) inhibitors and investigated the effect that the 14h inhibitor had on TSC2, S6K1, Rictor, S6 protein and 4EBP1 phosphorylation (Fig 7). Consistent with SGK3 mediating phosphorylation of TSC2 and leading to the activation of mTORC1 under these conditions, we observed that treatment with 3 μM 14h for 1 hour suppressed phosphorylation of TSC2. We also observed suppression of activity and phosphorylation of S6K1 and its downstream targets, Rictor and S6 protein (Fig 7A and 7B). However, phosphorylation of 4EBP1, other mTORC1 substrate, was not markedly reduced upon SGK3 inhibition (Fig 7A). In contrast, 14h did not inhibit TSC2, S6K1, Rictor, S6 protein or 4EBP1 phosphorylation or S6K1 activity in ZR-75-1 cells cultured in serum in the absence of prolonged treatment with PI3K or Akt inhibitors (Fig 7A and 7B). As expected, under these conditions Class I PI3K or Akt inhibitors suppressed TSC2, S6K1, Rictor, S6 protein or 4EBP1 protein phosphorylation as well as S6K1 activity (Fig7A) and addition of SGK inhibitor (14h) failed to ablate dephosphorylation of these substrates (SFig5). To further evaluate impact of SGK3 inhibition, we performed shRNA mediated knock-down of SGK3 expression in ZR-75-1 cells treated in the presence or absence of the Akt (MK-2206) inhibitor for 1hour or 5 days (Fig 7C). This revealed that knock-down of SGK3 markedly reduced phosphorylation of NDRG1 as well as TSC2, leading to an inhibition of mTORC1, reflected by the inhibition of S6K1, Rictor, S6 protein and 4EBP1 phosphorylation when compared to scrambled shRNA control samples (Fig 7C).

We also tested whether the addition of hVps34 inhibitor (VPS34-N1) would have the same suppressive effect on phosphorylation of TSC2 and mTORC1 substrates as SGK3 inhibition (SFig6). We found that addition of 1μM VPS34-IN1 for 1hour after prolonged treatment with Akt (MK-2206) or Class I PI3K (GDC0941) inhibitors had a similar effect as SGK3 inhibition (SFig6). We observed reduced phosphorylation of TSC2, S6K1, Rictor, S6 protein and 4EBP1 (SFig6). Treatment of ZR-75-1 cells for one hour with 1μM of VPS34-IN1 alone under conditions which SGK3 is not activated, did not have an effect on TSC2 or mTORC1 substrate phosphorylation.

To explore whether any other potential SGK3 phospho-substrates could be detected, we treated ZR-75-1 cells for 1 hour or 5 days with Akt inhibitor (MK-2206) or Class I PI3K (GDC0941) in the presence or absence of SGK3 inhibitor (14h) for one hour prior to lysis. Lysates were immunobloted with anti-p-Akt motif substrate antibody (RxRxxpS/pT) (Zhang et al, 2002) . The results revealed that at least 6 Akt substrates detected by the p-Akt motif antibody were re-phosphorylated on Akt phosphorylation consensus motif after a 5-day exposure to Akt (MK-2206) or Class I PI3K (GDC0941) inhibitors when SGK3 is upregulated, in a manner that was blocked by the 14h SGK3 inhibitor (SFig 7). We also observed 3 Akt substrates that were not re-phosphorylated on Akt phosphorylation consensus motif after a 5-day exposure to MK-2206/GDC0941 when SGK3 is upregulated, suggesting these are Akt selective (like PRAS40). No

evidence of any SGK3 selective substrates recognised by the p-Akt motif antibody was observed (SFig 7).

Combined inhibition of both Akt and SGK is required to regress BT-474 xenograft tumours.

In order to establish the therapeutic potential of combined AKT and SGK3 inhibition in a breast cancer model, we tested cell proliferation *in vitro* and established xenografts in nude mice with BT-474 cells, which are sensitive to Akt inhibitors when cultured in vitro (Sommer et al, 2013) and in which prolonged treatment with Akt inhibitors leads to upregulation of SGK3 (Fig 8A). Measurement of cell confluency over 5-6 days in the continued presence of the Akt inhibitors, MK2206 or AZD5363, revealed a dose dependent inhibition of cell growth compared to DMSO treated cells (Fig 8B upper and bottom panel, SFig 8A and 8B). Treatment with SGK inhibitor (14h) alone had little anti-proliferative effect, even at 3μM concentration (Fig 8B upper and bottom panel, SFig 8A and 8B). To determine whether a combination effect could be observed following prolonged inhibition of Akt, a long-term growth assay was undertaken. Culture in the presence of 0.3 μM Akt inhibitors (AZD5363 or MK-2206) dramatically slowed the growth of BT474c cells but they eventually reached confluency after approx 24 and 20 days, respectively. Addition of 3 μM SGK inhibitor (14h) induced further reduction in cell growth when it was combined with Akt inhibitor (AZD5363 or MK-2206) from the beginning of treatment or added sequentially 12 days after initial administration of Akt inhibitor (AZD5363 or MK-2206) alone (Fig 8B, upper and bottom panel).

The anti-tumour efficacy of the Akt (MK-2206) and SGK (14h) inhibitors as monotherapy and in combination was investigated in the BT-474 human breast xenograft model. At 100 mg/kg MK-2206 the in-vivo growth of BT-474 was inhibited at ~ 20% ($p<0.01$) however no regression as monotherapy was observed. No anti-tumour effects were observed following treatment with the SGK inhibitor alone (14h, 25 mg/kg). However, concomitant administration of both agents had a significantly greater effect than that observed with either agent alone, including ~ 80% regression in all tumours ($p<0.001$). No toxicity or weight loss relative to the vehicle control group was observed in any treatment group (Fig 8D). The concentration of inhibitors in the plasma measured 2-3 hours after the final administration was 1-3 μM (Fig 8E), without significant differences when administered as a monotherapy or combination. To evaluate whether tumour regression in combination treatment was due to apoptosis, we performed immunohistochemical analysis of tumour samples with anti-Cleaved Caspase3 antibodies. Results showed increased number of apoptotic cells in Akt inhibitor (MK-2206) monotreatment as compared to vehicle treatment and the number of apoptotic cells was significantly higher ($p<0.001$) in combination (MK-2206 and 14h) treatment compared to MK-2206 treatment alone (Fig 8F). Taken together, these data indicate that inhibition of both Akt and SGK is required to achieve superior anti-tumour activity in these xenografts.

To elucidate possible mechanisms for antiproliferative effect with SGK and Akt inhibitor combination treatment in *in vitro* and *in vivo* experiments, we analysed tumour samples taken at the end of the treatment. Immunohistochemical and

immunoblot analysis revealed that Akt inhibitor (MK-2206) alone ablated Akt 473 and PRAS40 phosphorylation and partially reduced NDRG1 phosphorylation and S6 protein phosphorylation (Fig 8G and 8H). SGK inhibitor (14h) when administered alone had no major effect on phosphorylation of any of these markers (Fig 8G and 8H). Combination of Akt and SGK inhibitors (MK-2206 and 14h) resulted in the ablation of NDRG1 phosphorylation and a more moderate inhibition of S6 protein phosphorylation than was observed with MK-2206 inhibitor alone (Fig 8G and 8H). Immunoblot analysis also revealed that SGK3 protein level was not markedly upregulated in tumours of mice treated with either Akt inhibitor (MK-2206) alone or in combination with SGK3 inhibitor (14h). However, the phosphorylation of NDRG (Thr246) was not ablated in Akt inhibitor treatment, indicating higher SGK3 activity, whereas combination treatment (MK-2206 and 14h) induced marked dephosphorylation of NDRG1 (Fig 8H). Additionally, phosphorylation of S6K1 (Thr389), S6 (Ser240/244) and 4EBP1 (Ser65) were detectable in samples of mice treated with Akt inhibitor (MK-2206) alone, while they were severely diminished in samples of mice receiving combination treatment (Fig 8H). These results indicate possible reactivation of the mTORC1 pathway after monotreatment with the Akt inhibitor (MK-2206). However, it is not clear whether the reactivation was mediated through SGK3 phosphorylating TSC2 at Akt sites (Thr1462), since the tumour samples obtained from monotreated (MK-2206) or combination (MK-2206 and 14h) mice showed similar level of TSC2 phosphorylation (Fig 8H). Further analysis of BT-474c cell line treated for 5 days with Akt inhibitor (MK-2206) and subsequent 1-hour treatment with SGK3 inhibitor (14h) showed the similar results as observed in ZR-75-1 cells. We observed suppression of phosphorylation of TSC2, S6K1 and its downstream target S6 protein (SFig. 9). Phosphorylation of 4EBP1, was not markedly reduced upon SGK3 inhibition (SFig 9). SGK inhibitor (14h) did not significantly suppress phosphorylation of TSC2, S6K1, S6 protein or 4EBP1 in BT-474c cells cultured in serum in the absence of prolonged treatment with Akt inhibitor (SFig9).

Exploitation of digital barcoding technology to quantify human kinome mRNA after inhibitor exposure

Given the profound effects of prolonged treatment with Akt and Class I PI3K inhibitors on SGK3 mRNA in cells, we next quantified the effects of MK-2206, AZD5363 and GDC0941 across the complete human protein kinase superfamily (Excel file 1). To accomplish this, we employed NanoString technology (Geiss et al, 2008) to digitally capture dynamics of the kinase transcriptome in response to all 3 compounds after 5 days of compound exposure (Fig 9). This data revealed complex reprogramming signatures and the appearance of compound-specific profiles. For example, exposure to MK-2206 (Fig.9A) and AZD5363 (Fig. 9B) both promoted an increase in RET and SGK110 (both from low basal levels), and a marked decrease in CDK6 mRNA levels. In contrast, exposure to the PI3K inhibitor GDC0941 (Fig. 9C) induced a more generalised kinome-wide increase in mRNA levels alongside a profound elevation in SGK3 mRNA. Indeed, out of the 536-member kinase panel, SGK3 mRNA had increased to become the 48th highest level of expression by day 5, compared to 230th in the matched DMSO control, 94th in MK-2206 and 144th in AZD5363. In contrast, we found that PKCγ mRNA

levels consistently decreased after exposure to all 3 inhibitors. These data revealed that although SGK1 and SGK2 were expressed at extremely low levels in ZR-75-1 cells (Excel file 1), very small drug-induced increases in SGK2 could be detected using a sensitive digital assay (Excel file 1). However, SGK2 increases were very low compared to SGK3 (Excel file 1), which had reached an expression level equivalent to ~0.5% of the entire kinome mRNA after GDC0941 exposure for 5 days.

The six human AKT and SGK protein kinases belong to the AGC kinase subfamily. To evaluate specific effects of Akt/PI3K inhibitors on the complete AGC family, we quantified actual and relative levels of the 60 human AGC kinases in triplicate samples after exposure to compounds for either 2 days (SFig. 10) or 5 days (SFig. 11). SGK3 was consistently the most highly up-regulated AGC kinase mRNA after exposure to all 3 compounds. Interestingly, the Akt inhibitors AZD5363 (2-3 fold up-regulation) or MK-2206 (4-5 fold up-regulation) were less potent inducers of SGK3 mRNA compared to GDC0941 (6-10-fold increase). Several other AGC kinases, including RSKL2 and MSK1, also demonstrated statistically-significant upregulation in response to several of these compounds (SFig. 10 and 11). The AGC kinome data set also provided the opportunity to assess relative absolute mRNA levels. Interestingly, AKT1 and AKT2 mRNA levels were the highest amongst all AGC kinases in ZR-75-1 cells under the conditions studied, consistent with a key endogenous pro-survival role. Consistent with our previous findings, exposure of ZR-75-1 cells to these inhibitors for either 2 or 5 days (SFig 10 and 11) had a specific and profound effect on SGK3 mRNA content. For example, SGK3 mRNA represented only the 29th most highly expressed AGC kinase in the presence of DMSO vehicle, but it had increased to become the 12th most highly abundant AGC kinase mRNA after exposure to MK-2206, and the 7th most highly abundant after exposure to GDC0941.

Discussion

Akt isoforms play crucial roles in regulating survival and proliferation of cancer cells and it would therefore be expected that loss of Akt activity resulting from prolonged treatment with Class I PI3K or Akt inhibitors would not be well tolerated. Such tumours would thus be under great therapeutic pressure to upregulate additional signalling pathways to compensate for this loss of Akt activity. The ability to rapidly upregulate the SGK3 pathway represents an ingenious solution, not only because SGK3 possesses similar substrate specificity as Akt and hence the ability to phosphorylate at least a subset of overlapping substrates, but also because SGK3 can be activated independently of Class I PI3K via hVps34. Therefore, upregulation of SGK3, which we observed in our models of Akt-sensitive breast cancer cell lines, could serve as a strategy to circumvent inhibition of Class I PI3K as well as Akt isoforms and provide adaptive resistance response. Indeed, immunoblot analysis of ZR-75-1 total cell extracts employing the p-Akt motif antibody suggested that 6 out of the 9 detected Akt substrates are likely to be phosphorylated by both Akt and SGK3 (SFig 7).

By virtue of its PX domain, SGK3 is capable of binding to PtdIns(3)P produced by hVps34 on the endosomes (Bago et al, 2014) and our biochemical data suggest

that PtdIns(3)P binding can directly promote phosphorylation and activation of SGK3 by PDK1 (Fig 4). However, it has also been reported that metabolism of PtdIns(3,4,5)P_3 to PtdIns(3)P at the plasma membrane via the consecutive actions of the SHIP2 and INPP4A/B inositol phosphatases can activate SGK3, and these conclusions are partially based on the findings that Class I PI3K inhibitors suppress SGK3 activity (Fig 2B) (Chi et al, 2015; Gasser et al, 2014). SGK3 is also partially suppressed by treatment with Class I PI3K inhibitors in U2OS cells (Bago et al, 2014). In our opinion it has not yet been possible to rule out whether the effect of Class I PI3K inhibitors on SGK3 activity is a consequence of these compounds inhibiting the activation of mTORC2 that triggers SGK3 activation by phosphorylating the hydrophobic motif rather than an effect on plasma membrane PtdIns(3)P levels generated via metabolism of PtdIns(3,4,5)P_3.

Other SGK isoforms (SGK1 or SGK2) do not possess a PX domain and, like Akt, are activated downstream of Class I PI3K isoforms. It would therefore be unlikely that SGK1 and SGK2 could substitute for Akt in cells treated with Class I PI3K inhibitors, which may explain why we did not observe marked upregulation of SGK1 or SGK2 in the experiments we undertook (Fig 1 & 2). The conserved emergence of SGK3 as a key inducible resistance determinant might potentially be explained by the very high endogenous levels of AKT1 and AKT2 expression already present in these cells, and the almost complete absence of AKT3, SGK1 and SGK2 mRNAs (Excel File 1) as potential compensatory mechanisms for when Akt1 and Akt2 activity are blocked.

The SGK3 gene has been reported to be an estrogen or androgen receptor transcriptional target in ER-positive breast cancer cells (Wang et al, 2011; Xu et al, 2012) and in androgen receptor (AR) positive prostate cancer (Wang et al, 2014). It would be important to investigate the molecular mechanism by which prolonged inhibition of Akt or Class I PI3K leads to kinome-wide changes in mRNA expression levels, and in particular SGK3 mRNA and whether the upregulation of SGK3 protein and activity is limited to ER/AR cell backgrounds/tumours, or applicable to broader group of cancer cells. It would also be interesting to perform kinome-wide mRNA profiling in a wide selection of tumour or patient-derived cells before and after inhibitor exposure, so that drug resistance signatures in addition to SGK3 can be compared and contrasted as potential guides to inform targeted therapeutics.

The notion that SGK isoforms can play an important role in controlling growth and proliferation is also supported by research undertaken in model organisms such as *Caenorhabditis elegans* and budding yeast. Studies in *Caenorhabditis elegans* reveal that SGK rather than Akt is the key mediator of proliferation responses by controlling fat metabolism, reproduction and life-span (Jones et al, 2009; Soukas et al, 2009). In budding yeast, the SGK homologues termed YPK1 and YPK2 also play a vital role in regulating metabolic and other responses required for viability and proliferation (Casamayor et al, 1999; Niles et al, 2012). Previous work has shown that SGK3 is overexpressed in a variety of cancer cell lines and knock-down of SGK3 in these cells including in ZR-75-1 cells employed in this study has substantial impact on proliferation (Chi et al, 2015; Gasser et al,

2014; Virbasius et al, 2001), results we have been able to confirm (RB, data not shown).

Our data reveal that by phosphorylating TSC2 and activating mTORC1, SGK3 can mediate what has previously been referred to as "Akt-independent signalling" (Bruhn et al, 2010; Bruhn et al, 2013). It is likely that in addition to TSC2, SGK3 will phosphorylate a group of Akt substrates that could play important roles in driving metabolic, transcription, and translational responses needed for the survival and proliferation of cancer cells. Consistent with this, 6 out of the 9 Akt substrates detected immunoblot analysis of ZR-75-1 cell extracts appear to be phosphorylated by both Akt and SGK3 (SFig 7). However, it should be noted that SGK3 does not phosphorylate PRAS40 (Thr246) or Foxo1 (Ser256) (Fig 6), indicating that a subset of Akt substrates are likely not phosphorylated by SGK3. In these studies we did not detect any SGK3 selective substrates that are not phosphorylated by Akt (SFig 7). Further work would be required to understand the mechanisms determining whether Akt substrates can be phosphorylated by SGK3, but this could be controlled by consensus motif sequences and/or cellular localisation of the substrate could be an important determinant.

We also noticed that under conditions of sustained Akt inhibition in ZR-75-1 cells, in which SGK3 is activated, addition of SGK3 inhibitor (14h) (Fig 7A), whilst suppressing S6K1 phosphorylation, failed to commensurately reduce 4EBP1 phosphorylation. Similar results have been observed in other cell lines treated with the mTORC1 inhibitor rapamycin or starved from amino acids, where S6K1 phosphorylation was suppressed to a much greater extent than 4EBP1 (Choo et al, 2008; Kang et al, 2013). Other mTORC1 substrates have also been reported to be differentially affected following inhibition of mTORC1 (Kang et al, 2013). It has been suggested that this results from mTORC1 substrates being deferentially sensitive to residual mTORC1 activity depending on the type and the duration of the stress conditions (Kang et al, 2013). We have also observed that the hVps34 inhibition leads to a greater dephosphorylation of 4EBP-1 than seen with SGK3 inhibition (SFig 6). This could be accounted for if the inhibition of hVps34 led to suppression of mTORC1 through mechanisms additional to SGK3. Indeed, several studies report regulation of mTORC1/S6K1 by hVps34 in response to amino acid starvation through an ill-defined mechanism (Byfield et al, 2005; Nobukuni et al, 2005). We also observed that in BT-474c cells, the inhibition of SGK3 induced a more moderate inhibition of S6K1 than in ZR-75-1 cells (Fig 6 & SFig 9), indicating that there is likely to be variation between cancer cell lines.

In this study we have further characterized 14h, a novel small-molecule cell-permeant SGK inhibitor initially reported by Sanofi (Halland et al, 2015). 14 h and the other related inhibitors we have analysed (14g, 14i and 14n) are much more specific than a previously reported and widely used SGK inhibitor GSK650394 (Sherk et al, 2008) that inhibits many kinases other than SGK1 (http://www.kinase-screen.mrc.ac.uk/screening-compounds/348807?order=field_results_inhibition&sort=asc). The only other relatively selective SGK1 inhibitor that we are aware of, EMD638683 (http://www.kinase-screen.mrc.ac.uk/screening-compounds/617594) is not potent displaying an in vitro IC50 of only 3 μM (Ackermann et al, 2011).

Consistent with this, extremely high doses of 100 μM EMD638683, are required to observe marginal reduction of NDRG1 phosphorylation in breast cancer cells that express high levels of SGK1 (Eeva Sommer data not shown). Our data demonstrate that 1 to 3 μM 14h, optimally suppresses SGK3 mediated phosphorylation of NDRG1 and TSC2 in cells (Fig 5 to 7). We also observed that 14h in addition to inhibiting SGK3 catalytic activity also suppressed phosphorylation of both the T-loop and hydrophobic motif of SGK3 in cells (Fig 5E), as well as inhibiting PDK1 from phosphorylating SGK3[S486E] in the presence of PtdIns(3)P in vitro (Fig 5F). This is analogous to Akt allosteric inhibitors such as MK-2206 that interact in an interface between the PH domain and the kinase domain, trapping Akt in a conformation that cannot be activated by PDK1 and mTORC2 (Calleja et al, 2009; Green et al, 2008; Wu et al, 2010). 14h was expected to function as a conventional Akt competitive inhibitor (Halland et al, 2015), so it is unusual for this compound to also work by preventing the activation of SGK3 by its upstream activators.

The finding that the growth of BT-474 breast cancer cells in in vitro and in a xenograft model is highly sensitive to a combination of Akt (MK-2206) and SGK (14h) inhibitors that induced inhibition of cell growth and tumour regression emphasises the therapeutic potential of a strategy of targeting both the Akt and SGK kinases for the treatment of cancer. We cannot rule out that 14h has off-target effects in a xenograft model and it would be critical to repeat these studies with a structurally diverse SGK inhibitor when it becomes available. Also, it would be useful to analyse the sensitivity of a broader number of tumours to combinations of SGK and Akt or Class I PI3K inhibitors.

In conclusion, our findings highlight the critical importance of the hVps34-SGK3 pathway and reveal that this upregulated signalling module represents a major mechanism that cells utilise to counteract inhibition of the PI3K-Akt signalling network. SGK3 is consistently the most highly up-regulated kinase mRNA amongst the 60 human AGC kinases evaluated in ZR-75-1 cells exposed to either Class I PI3K or Akt inhibitors. Our findings also reveal the hVps34-SGK3 signalling pathway operates as a PI3K-Akt independent network to stimulate mTORC1 and likely other pathways that promote cancer growth. We demonstrate that sustained suppression of Class I PI3K or Akt activity over several days triggers the selective upregulation of SGK3 mRNA and protein as well as its catalytic activity in a variety of breast cancer cell lines. Our results suggest that SGK3 is specifically activated by the hVps34 lipid kinase that generates PtdIns(3)P on endosomal membranes. PtdIns(3)P then binds to the PX domain of SGK3, promoting its phosphorylation and activation by PDK1. Our findings indicate that once activated in cells that lack Akt activity, SGK3 substitutes for Akt by phosphorylating TSC2 to trigger activation of mTORC1. Our characterisation of the 14h SGK inhibitor suggests that it will become a useful research tool to probe signalling responses controlled by SGK isoforms in vivo. 14h represents a valuable addition to our growing armoury of signal transduction inhibitors to dissect functional roles of protein kinases. Finally, we establish that combined administration of Akt (MK-2206) and SGK (14h) inhibitors to mice bearing xenograft BT-474 breast cancer tumours induces a striking tumour regression compared to when the inhibitors were administered

individually. These findings highlight the therapeutic potential of a strategy targeting both the Akt and SGK kinases for the treatment of cancer.

MATERIALS AND METHODS

Materials. Protein-G Sepharose, Glutathione-Sepharose (Amersham Biosciences); [γ-^{32}P]ATP (Perkin Elmer); Triton X-100, EDTA, EGTA, sodium orthovanadate, sodium –glycerophosphate, sodium fluoride, sodium pyrophosphate, 2- mercaptoethanol, sucrose, benzamidine ,Tween-20, Tris-HCl, sodium chloride, magnesium acetate, DMSO, reduced glutathione (Sigma); phenylmethylsulfonyl fluoride (PMSF) (Melford); tissue culture reagents, Novex 4-12% Bis-Tris gels, NuPAGE LDS sample buffer 4x (Invitrogen); Ampicillin (Merck); P81 phosphocellulose paper (Whatman); methanol (VWR Chemicals). liver phosphatidylcholine, brain phosphatidylserine, 1,2-dioleoyil-sn-glycero-3 (phosphoinositol-3-phosphate) and 1,2-dioleoyl-sn-glycero-3-phosphoinositol (Avanti Polar Lipids). Inhibitors GDC0941 (Axon Medchem), BKM120 (ChemieTek), MK-2206 (Selleck), GSK2334470 (Tocris), AZD8055 (Selleck) were purchased from the indicated suppliers. AstraZeneca provided AZD5363. VPS34-IN1 was synthesized as described in Bago *et al*. SAR405 (CAS: 1523406-39-4) was synthesized as described in Ronan B. *et al.* Sanofi compounds 14g, 14h, 14i and 14n were synthesized as described previously (Halland et al, 2015). All recombinant proteins, DNA constructs, antibodies and inhibitors including VPS34-IN1 and SAR405 generated for the present study are described and can be requested on our reagents website (https://mrcppureagents.dundee.ac.uk/).

General methods. DNA procedures were undertaken using standard protocols. DNA constructs were purified from E.coli DH5alpha using maxi prep kit (Quiagen). DNA sequence of the DNA constructs used in this study was performed by the Sequencing Service (MRC Protein Phosphorylation Unit, College of Life Sciences, University of Dundee, UK; www.dnaseq.co.uk).

Antibodies. The following antibodies were raised in sheep, by the Division of Signal Transduction Therapy (DSTT) at the University of Dundee, and affinity-purified against the indicated antigens: anti-Akt1 (S695B, third bleed; raised against residues 466–480 of human Akt1: RPHFPQFSYSASGTA), anti-NDRG1 (S276B third bleed; raised against full-length human NDRG1) (DU1557), anti-SGK3 (S037D second bleed; raised against human SGK3 PX domain comprising residues 1–130 of SGK3) (DU2034), anti-PDK1 (S682, third bleed; raised against residues 544–556 of human PDK1: RQRYQSHPDAAVQ) and anti-S6K1 (S417B, 2nd bleed; raised against residues 25-44 of human S6K1: AGVFDIDLDQPEDAGSEDEL). Anti-phospho-Akt Ser473 (#9271), anti-phospho-Akt Thr308 (#4056), anti-phospho-NDRG1 Thr346 (#5482), anti-GAPDH (#2118), anti-phospho-TSC2 Thr1462(#3617), anti-phospho-TSC2 Ser939 (#3615), anti-TSC2 (#3612), anti-phospho-Rictor Thr1135 (#3806), anti-Rictor (#2140), anti-phospho- S6K1 Thr389 (#9205), anti- phospho-rpS6 Ser240/244 (#2215), anti-phospho-rpS6 Ser235/36 (#4856), anti-rpS6 (#2217), anti-phospho-4EBP1 Ser65 (#9451), anti-4EBP1 (#9452), anti-phospho- SGK3 Thr320 (#5642) and anti-phospho-Akt substrate (RxRxxS/T) (#10001) antibodies were purchased from Cell Signalling Technology. Anti-(phospho-SGK hydrophobic motif [Ser486 in SGK3]) antibody (#sc16745) was from Santa Cruz Biotechnology and total anti-SGK antibody was from Sigma (#5188). Secondary antibodies coupled to HRP (horseradish peroxidase) were obtained from

Thermo Scientific.

Cell culture and cell lysis. ZR-75-1, CAMA-1, T47D and BT-474c cell lines were sourced as described previously (Davies et al, 2012). HEK 293 cells were purchased from the American Tissue Culture Collection (ATCC). Cells were cultured in RPMI or DMEM media supplemented with 10% (v/v) foetal bovine serum, 2 mM L- glutamine, 100U/ml penicillin and 0.1 mg/ml streptomycin. Inhibitor treatments were carried out as described in figure legends. During five days inhibitor treatments the media was changed after 72-hour intervals. The cells were lysed in buffer containing 50 mM Tris-HCl (pH 7.5), 150 mM NaCl, 1 mM EDTA, 1 mM EGTA, 1 mM sodium orthovanadate, 10 mM sodium - glycerophosphate, 10 mM sodium pyrophosphate, 0.27 M sucrose, 0.1% (v/v) 2-mercaptoethanol, 1 mM benzamidine and 0.1 mM PMSF. Lysates were clarified by centrifugation at 16,000g for 10 min at 4^{o}C. Protein concentration was calculated using Bradford assay (Thermo Scientific). Immunoblotting and immunoprecipitation were performed using standard procedures. The signal was developed using ECL Western Blotting Detection Kit (Amersham) on Amersham Hyperfilm ECL film (Amersham).

Real-time PCR for SGK1, SGK2 and SGK3.Total RNA was isolated using RNA extraction kit (Qiagen) and cDNA was prepared using iSsript cDNA synthesis Kit (BIO-RAD) according to manufacturer's instructions. PCR reactions were done in 20 µL volume, containing 5 µL cDNA, 0.5 µM each primer (Invitrogen), and SSsoFast Eva Green Supermix (BIO-RAD). All PCR reactions were run as follows: 95°C for 5 min, followed by 45 cycles at 95°C for 5 s, 60°C for 30 s. Each sample was run in triplicate in three independent experiments. 2^(-deltadelta) Ct method was used to calculate relative mRNA expression. C_t values were normalized against 18sRNA and relative expression was calculated using DMSO treated cDNA sample as a calibrator. Primers used in this study were as follows : SGK1 sense: 5'CTAACGTCTTTCTGTCTC'3 and antisense: 5'CATAGGAGTTATTGGCAAT'3, SGK2 sense: 5'CTTCCATCTCACTAACCA'3 and antisense: 5'CTTTGTTATTAGGGATAGTCA'3, SGK3 sense: 5'GAAGTGAATGGTTTGTCT'3 and antisense:5'ATATTCTCTTGCCAGGAA'3 and 18S sense: 5'AATGGCTCATTAAATCAGTT and antisense: 5'CTAGAATTACCACAGTTATCC'3.

SGK3 and Rictor knock-down and cell transfection. SGK3 knock-down was performed by using the MISSION shRNA (Sigma Aldrich) pLKO.1 vectors. Rictor knock-down shRNA sequence (insert sequence: ACCGGACTTGTGAAGAATCGTATCTTCTCGAGAAGATACGATTCTTCACAAGTTTTTTGAATTC) was cloned in pLKO1-puro vector (DU44740). Lentiviruses were produced in HEK293T cells, by transfecting 70% confluent 15 cm tissue culture dish with 10 µg DNA (8 µg shRNA-pLKO1-puro, 4 µg pCMVdelta R8.2 packaging vector (Adgene) and 2 µg pCMV-VSV-G envelope vector (Adgene)). DNA was mixed with 40 µL of polyethylenimine in 300 µL Optimem media (Invitrogen). The media containing viruses was collected and filtered 48 hours after transfection. Breast cancer cell lines were kept in virus containing media for 24 hours. Cells were allowed to recover in fresh media for 24 hours, before the

media was replaced with the selection media containing puromycin (2 μg/ml). The cells were kept in selection media for ten days before using for the experiments, unless stated otherwise.

Immunoprecipitation and assay of SGK3, Akt and S6K1. *In vitro* kinase activity of SGK3, Akt and S6K1 was assayed as described previously (Bago et al, 2014). Briefly, SGK3, Akt and S6K1 were immunoprecipitated from 1mg ZR-75-1 cell lysate. Immunoprecipitates were washed in sequence with lysis buffer containing high salt concentration (500 mM NaCl), lysis buffer and Buffer A (50 mM Tris pH7.5, 0.1mM EGTA). Kinase activity was assessed by measuring [γ-^{32}P]ATP incorporation into Crosstide substrate peptide [GRPRTSSFAEGKK]. The reactions were carried in 40 μL total volume containing 0.1 mM[γ-^{32}P]ATP(400-1000 cpm/pmol), 10 mM magnesium acetate and 30 μM Crosstide peptide. Reactions were terminated by adding 10 μL 0.1 M EDTA and spotting 40 μL of the resulting reaction mix on P81 paper, which were immediately immersed into 50 mM orthophosphoric acid. Papers were washed at least five times in 50 mM orthophosphoric acid, rinsed in acetone and air dried. Radioactivity was quantified by Cerenkov counting. One unit of enzyme activity was defined as amount of enzyme that catalyses incorporation of 1 nmol of [γ-^{32}P]ATP into the substrate over one minute.

Production of recombinant SGK3. SGK3 [S486E]-GST (DU 52370) and SGK3 [R90A S486E]-GST (DU52372) in pCMV5D vector were transfected in HEK293 cells using polyethylenimine. The cells were lysed 48 hours post transfection in the lysis buffer without phosphatase inhibitors following 1-hour incubation in the presence of PDK1 inhibitor (GSK2334470, 5 μM) and hVps34 inhibitor (VPS34-IN1, 5 μM). The lysates were clarified by centrifugation and GST-tagged proteins were affinity purified using GST-Sepharose beads. The proteins were eluted with 40 mM glutathione, pH 8.0, aliquoted and stored at -80°C.

SGK3 kinase assay on phospholipid vesicles. Lipid vesicles were prepared as described in (Alessi et al, 1997b). Briefly, the mixture containing 1 mM phosphatidlycholine, 1 mM phosphatidylserine and either 0.01 to 0.1 mM phosphatidylinositol or 0.01 to 0.1 mM phosphatidylinositol(3) phosphate in chloroform was dried under vacuum and further resuspended in kinase assay buffer (10 mM Tris –HCl, pH 7.4, 150 mM NaCl, 0.1 mM EGTA) by vortexing and sonication. Multilamellar vesicles formed in this process were passed through 0.2 μm filter using lipid extruder, after which a suspension of smaller unilamellar vesicles was obtained. Solutions were stored at 4°C at concentrations 10x higher than those used in the kinase assay and used within 3 days. The kinase assay was carried out in two stages; in the first stage 50 ng of SGK3 [S486E]-GST or SGK3 [R90A, S486E]-GST was incubated with lipid vesicles, 10 mM Mg-acetate and 0.1 mM ATP. The reaction was started by adding 50 ng of recombinant GST-PDK1 (32U/mg) (DU954) to permit activation of SGK3-GST. After 30 min at 30°C, the reaction was stopped by adding PDK1 inhibitor (GSK2334470, 1μM). In the second stage, the reaction mixture was topped up with 0.1 mM ATP and reaction started by adding 2 μg of recombinant GST-NDRG1 (DU1557) to permit phosphorylation by activated SGK3-GST. The assay was carried out for 30 min at 30°C. The reaction was stopped by adding 4x LDS sample buffer.

Determination cell growth *in vitro*. For growth assays BT474c cells were seeded in 12-well plates at a density of $1x10^5$ cells/well and left to adhere overnight. Cells were then treated with MK-2206, AZD5363 and 14h inhibitors. and imaged every 4 hours on the Incucyte ZOOM (Essen Bioscience) for up to 4 weeks to give a measure of cell confluency. Media was refreshed every 4-5 days. Inhibitor treatments were carried out as described in figure legends

Animal studies and IHC. Experiments involving mice were in accordance with Institutional Guidelines of Memorial Sloan Kettering Cancer Center (Protocol number 12-10-019). Animals were housed in air-filtered laminar flow cabinets with a 12-hour light cycle and food and water *ad libitum*. BT-474 VH2 (Baselga et al, 1998) were resuspended in 1:1 Complete media/Matrigel (Corning) and injected subcutaneously into the flanks of six-week-old female athymic *Foxn1*^{nu} nude mice (Harlan Laboratories). Animals' drinking water was supplemented with 1 μM 17β-E2 (Sigma). When tumours reached a volume of ~150mm^3, mice were randomized, treated, and tumours were measured twice a week. Tumour volume was determined using the following formula: (length × width^2) ÷ 2. Tumour growth was represented as the fold change mean ± SEM. Treatments were as follows: MK-2206 (100 mg × kg^{-1} in 30% Captisol (Sigma), 5 times/week, p.o.) and 14h (25 mg × kg^{-1} in 40% of 3:1 Glycofurol/Kolliphor® RH 40 mixture (Sigma) in 0.9% saline, 5 times/week, p.o.). Tumours were harvested at the end of the experiment four hours after the last dosage, fixed in 4% formaldehyde in PBS, and paraffin-embedded. IHC was performed on a Ventana Discovery XT processor platform using standard protocols and the following antibodies from Cell Signalling Technology: pAkt(S473) (#4060), 1:70; pPRAS40(T246) (#2997), 1:50; pS6 (S240/4) (#5364),1:500; pNDRG1 (T346) (#5482), 1:200; Cleaved Caspase-3 (#9664), 1:50. Primary staining was followed by 60 minutes incubation with biotinylated goat anti-rabbit IgG (Vector labs) 1:200. Blocker D, Streptavidin- HRP and DAB detection kit (Ventana Medical Systems) were used according to the manufacturer instructions.

NanoString analysis. ZR-75-1 cells were collected, washed in PBS and snap-frozen. Cell pellets were resuspended at a concentration of ~6,500 cells/μl in RLT buffer (Qiagen). The equivalent of ~10,000 cells (~1.5 μl) were employed for direct kinase mRNA quantification, without the need for further mRNA purification or amplification. mRNAs were hybridised to NanoString human kinome barcode probes and control code sets, and kinase mRNA levels quantified using the nCounter colour barcoding system after count normalisation with internal housekeeping genes and 8 negative controls. For total copy numbers, triplicate normalised count values were averaged, and to calculate fold-induction, means were divided by triplicate mean values from matched DMSO controls. p-values were calculated using unpaired T-test (GraphPad Prism software) by employing treated and control count data for each kinase mRNA

Protein kinase profiling. Protein kinase profiling against Dundee panel of 140 protein kinases was undertaken at the International Centre for Protein Kinase Profiling. The result for each kinase was presented as a mean kinase activity of the reaction taken in triplicate relative to a control sample treated with DMSO.

Assay conditions and abbreviations are available at http://www.kinase-screen.mrc.ac.uk.

Statistical analysis. All experiments presented in this paper were performed at least twice and similar results were obtained. Error bars indicate standard deviation.

Acknowledgements
We thank Aaron Smith (AstraZeneca, R&D, Innovative Medicines) for measuring plasma MK-2206 and 14h concentrations in mouse xenografts and express gratitude to for the excellent technical support of the MRC-Protein Phosphorylation and Ubiquitylation Unit (PPU) DNA Sequencing Service (coordinated by Nicholas Helps), the MRC-PPU tissue culture team (coordinated by Kirsten Airey and Janis Stark), the Division of Signal Transduction Therapy (DSTT) antibody purification teams (coordinated by Hilary McLauchlan and James Hastie). This work was supported by the Medical Research Council (MC_UU_12016/3) and the pharmaceutical companies supporting the Division of Signal Transduction Therapy Unit (AstraZeneca, Boehringer-Ingelheim, GlaxoSmithKline, Merck KGaA, Janssen Pharmaceutica and Pfizer). We acknowledge NWCR for funding (project grants CR1037 and CR1088). The authors declare that they have no conflict of interest.

References

Ackermann TF, Boini KM, Beier N, Scholz W, Fuchss T, Lang F (2011) EMD638683, a novel SGK inhibitor with antihypertensive potency. Cell Physiol Biochem 28**:** 137-146

Alessi DR, Caudwell FB, Andjelkovic M, Hemmings BA, Cohen P (1996) Molecular basis for the substrate specificity of protein kinase B; comparison with MAPKAP kinase-1 and p70 S6 kinase. FEBS Lett 399**:** 333-338

Alessi DR, Deak M, Casamayor A, Caudwell FB, Morrice N, Norman DG, Gaffney P, Reese CB, MacDougall CN, Harbison D et al (1997a) 3-Phosphoinositide-dependent protein kinase-1 (PDK1): structural and functional homology with the Drosophila DSTPK61 kinase. Curr Biol 7**:** 776-789

Alessi DR, James SR, Downes CP, Holmes AB, Gaffney PR, Reese CB, Cohen P (1997b) Characterization of a 3-phosphoinositide-dependent protein kinase which phosphorylates and activates protein kinase Balpha. Curr Biol 7**:** 261-269

Backer JM (2008) The regulation and function of Class III PI3Ks: novel roles for Vps34. Biochem J 410**:** 1-17

Bago R, Malik N, Munson MJ, Prescott AR, Davies P, Sommer E, Shpiro N, Ward R, Cross D, Ganley IG et al (2014) Characterization of VPS34-IN1, a selective inhibitor of Vps34, reveals that the phosphatidylinositol 3-phosphate-binding SGK3 protein kinase is a downstream target of class III phosphoinositide 3-kinase. Biochem J 463**:** 413-427

Baselga J, Norton L, Albanell J, Kim YM, Mendelsohn J (1998) Recombinant humanized anti-HER2 antibody (Herceptin) enhances the antitumor activity of paclitaxel and doxorubicin against HER2/neu overexpressing human breast cancer xenografts. Cancer Res 58**:** 2825-2831

Bauer TM, Patel MR, Infante JR (2015) Targeting PI3 kinase in cancer. Pharmacol Ther 146**:** 53-60

Bendell JC, Rodon J, Burris HA, de Jonge M, Verweij J, Birle D, Demanse D, De Buck SS, Ru QC, Peters M et al (2012) Phase I, dose-escalation study of BKM120, an oral pan-Class I PI3K inhibitor, in patients with advanced solid tumors. J Clin Oncol 30**:** 282-290

Biondi RM, Kieloch A, Currie RA, Deak M, Alessi DR (2001) The PIF-binding pocket in PDK1 is essential for activation of S6K and SGK, but not PKB. EMBO J 20**:** 4380-4390.

Bruhn MA, Pearson RB, Hannan RD, Sheppard KE (2010) Second AKT: the rise of SGK in cancer signalling. Growth Factors 28**:** 394-408

Bruhn MA, Pearson RB, Hannan RD, Sheppard KE (2013) AKT-independent PI3-K signaling in cancer - emerging role for SGK3. Cancer Manag Res 5**:** 281-292

Brunet A, Park J, Tran H, Hu LS, Hemmings BA, Greenberg ME (2001) Protein kinase SGK mediates survival signals by phosphorylating the forkhead transcription factor FKHRL1 (FOXO3a). Mol Cell Biol 21**:** 952-965

Byfield MP, Murray JT, Backer JM (2005) hVps34 is a nutrient-regulated lipid kinase required for activation of p70 S6 kinase. The Journal of biological chemistry 280**:** 33076-33082

Calleja V, Laguerre M, Parker PJ, Larijani B (2009) Role of a novel PH-kinase domain interface in PKB/Akt regulation: structural mechanism for allosteric inhibition. PLoS Biol 7**:** e17

Cantley LC (2002) The phosphoinositide 3-kinase pathway. Science 296**:** 1655-1657.

Casamayor A, Torrance PD, Kobayashi T, Thorner J, Alessi DR (1999) Functional counterparts of mammalian protein kinases PDK1 and SGK in budding yeast. Curr Biol 9**:** 186-197

Chi MN, Guo ST, Wilmott JS, Guo XY, Yan XG, Wang CY, Liu XY, Jin L, Tseng HY, Liu T et al (2015) INPP4B is upregulated and functions as an oncogenic driver through SGK3 in a subset of melanomas. Oncotarget 6**:** 39891-39907

Choo AY, Yoon SO, Kim SG, Roux PP, Blenis J (2008) Rapamycin differentially inhibits S6Ks and 4E-BP1 to mediate cell-type-specific repression of mRNA translation. Proc Natl Acad Sci U S A 105**:** 17414-17419

Collins BJ, Deak M, Arthur JS, Armit LJ, Alessi DR (2003) In vivo role of the PIF-binding docking site of PDK1 defined by knock-in mutation. EMBO J 22**:** 4202-4211.

Collins BJ, Deak M, Murray-Tait V, Storey KG, Alessi DR (2005) In vivo role of the phosphate groove of PDK1 defined by knockin mutation. J Cell Sci 118**:** 5023-5034

Dai F, Yu L, He H, Chen Y, Yu J, Yang Y, Xu Y, Ling W, Zhao S (2002) Human serum and glucocorticoid-inducible kinase-like kinase (SGKL) phosphorylates glycogen syntheses kinase 3 beta (GSK-3beta) at serine-9 through direct interaction. Biochem Biophys Res Commun 293**:** 1191-1196

Davies BR, Greenwood H, Dudley P, Crafter C, Yu DH, Zhang J, Li J, Gao B, Ji Q, Maynard J et al (2012) Preclinical pharmacology of AZD5363, an inhibitor of AKT: pharmacodynamics, antitumor activity, and correlation of monotherapy activity with genetic background. Molecular cancer therapeutics 11**:** 873-887

Folkes AJ, Ahmadi K, Alderton WK, Alix S, Baker SJ, Box G, Chuckowree IS, Clarke PA, Depledge P, Eccles SA et al (2008) The identification of 2-(1H-indazol-4-yl)-6-(4-methanesulfonyl-piperazin-1-ylmethyl)-4-morpholin-4-yl-t hieno[3,2-

d]pyrimidine (GDC-0941) as a potent, selective, orally bioavailable inhibitor of class I PI3 kinase for the treatment of cancer. J Med Chem 51**:** 5522-5532

Garcia-Martinez JM, Alessi DR (2008) mTOR complex 2 (mTORC2) controls hydrophobic motif phosphorylation and activation of serum- and glucocorticoid-induced protein kinase 1 (SGK1). Biochem J 416**:** 375-385

Gasser JA, Inuzuka H, Lau AW, Wei W, Beroukhim R, Toker A (2014) SGK3 mediates INPP4B-dependent PI3K signaling in breast cancer. Mol Cell 56**:** 595-607

Geiss GK, Bumgarner RE, Birditt B, Dahl T, Dowidar N, Dunaway DL, Fell HP, Ferree S, George RD, Grogan T et al (2008) Direct multiplexed measurement of gene expression with color-coded probe pairs. Nat Biotechnol 26**:** 317-325

Gillooly DJ, Morrow IC, Lindsay M, Gould R, Bryant NJ, Gaullier JM, Parton RG, Stenmark H (2000) Localization of phosphatidylinositol 3-phosphate in yeast and mammalian cells. EMBO J 19**:** 4577-4588

Green CJ, Goransson O, Kular GS, Leslie NR, Gray A, Alessi DR, Sakamoto K, Hundal HS (2008) Use of Akt inhibitor and a drug-resistant mutant validates a critical role for protein kinase B/Akt in the insulin-dependent regulation of glucose and system A amino acid uptake. The Journal of biological chemistry 283**:** 27653-27667

Halland N, Schmidt F, Weiss T, Saas J, Li Z, Czech J, Dreyer M, Hofmeister A, Mertsch K, Dietz U et al (2015) Discovery of N-[4-(1H-Pyrazolo[3,4-b]pyrazin-6-yl)-phenyl]-sulfonamides as Highly Active and Selective SGK1 Inhibitors. ACS Med Chem Lett 6**:** 73-78

Hirai H, Sootome H, Nakatsuru Y, Miyama K, Taguchi S, Tsujioka K, Ueno Y, Hatch H, Majumder PK, Pan BS et al (2010) MK-2206, an allosteric Akt inhibitor, enhances antitumor efficacy by standard chemotherapeutic agents or molecular targeted drugs in vitro and in vivo. Molecular cancer therapeutics 9**:** 1956-1967

Jones KT, Greer ER, Pearce D, Ashrafi K (2009) Rictor/TORC2 Regulates Caenorhabditis elegans Fat Storage, Body Size, and Development through sgk-1. PLoS Biol 7**:** e60

Kang SA, Pacold ME, Cervantes CL, Lim D, Lou HJ, Ottina K, Gray NS, Turk BE, Yaffe MB, Sabatini DM (2013) mTORC1 phosphorylation sites encode their sensitivity to starvation and rapamycin. Science 341**:** 1236566

Kobayashi T, Cohen P (1999) Activation of serum- and glucocorticoid-regulated protein kinase by agonists that activate phosphatidylinositide 3-kinase is mediated by 3- phosphoinositide-dependent protein kinase-1 (PDK1) and PDK2. Biochem J 339**:** 319-328

Kobayashi T, Deak M, Morrice N, Cohen P (1999) Characterization of the structure and regulation of two novel isoforms of serum- and glucocorticoid-induced protein kinase. Biochem J 344**:** 189-197

Liu P, Cheng H, Roberts TM, Zhao JJ (2009) Targeting the phosphoinositide 3-kinase pathway in cancer. Nat Rev Drug Discov 8**:** 627-644

Liu P, Gan W, Chin YR, Ogura K, Guo J, Zhang J, Wang B, Blenis J, Cantley LC, Toker A et al (2015) PtdIns(3,4,5)P3-dependent Activation of the mTORC2 Kinase Complex. Cancer Discov

Manning BD, Tee AR, Logsdon MN, Blenis J, Cantley LC (2002) Identification of the tuberous sclerosis complex-2 tumor suppressor gene product tuberin as a target of the phosphoinositide 3-kinase/akt pathway. Mol Cell 10**:** 151-162.

Menon S, Dibble CC, Talbott G, Hoxhaj G, Valvezan AJ, Takahashi H, Cantley LC, Manning BD (2014) Spatial control of the TSC complex integrates insulin and nutrient regulation of mTORC1 at the lysosome. Cell 156**:** 771-785

Mora A, Komander D, Van Aalten DM, Alessi DR (2004) PDK1, the master regulator of AGC kinase signal transduction. Semin Cell Dev Biol 15**:** 161-170

Murray JT, Cummings LA, Bloomberg GB, Cohen P (2005) Identification of different specificity requirements between SGK1 and PKBalpha. FEBS Lett 579**:** 991-994

Najafov A, Shpiro N, Alessi DR (2012) Akt is efficiently activated by PIF-pocket- and PtdIns(3,4,5)P3-dependent mechanisms leading to resistance to PDK1 inhibitors. Biochem J 448**:** 285-295

Najafov A, Sommer EM, Axten JM, Deyoung MP, Alessi DR (2011) Characterization of GSK2334470, a novel and highly specific inhibitor of PDK1. Biochem J 433**:** 357-369

Niles BJ, Mogri H, Hill A, Vlahakis A, Powers T (2012) Plasma membrane recruitment and activation of the AGC kinase Ypk1 is mediated by target of rapamycin complex 2 (TORC2) and its effector proteins Slm1 and Slm2. Proc Natl Acad Sci U S A 109**:** 1536-1541

Nobukuni T, Joaquin M, Roccio M, Dann SG, Kim SY, Gulati P, Byfield MP, Backer JM, Natt F, Bos JL et al (2005) Amino acids mediate mTOR/raptor signaling through activation of class 3 phosphatidylinositol 3OH-kinase. Proc Natl Acad Sci U S A 102**:** 14238-14243

Pearce LR, Komander D, Alessi DR (2010) The nuts and bolts of AGC protein kinases. Nature reviews Molecular cell biology 11**:** 9-22

Rodon J, Dienstmann R, Serra V, Tabernero J (2013) Development of PI3K inhibitors: lessons learned from early clinical trials. Nat Rev Clin Oncol 10**:** 143-153

Ronan B, Flamand O, Vescovi L, Dureuil C, Durand L, Fassy F, Bachelot MF, Lamberton A, Mathieu M, Bertrand T et al (2014) A highly potent and selective Vps34 inhibitor alters vesicle trafficking and autophagy. Nat Chem Biol 10**:** 1013-1019

Sarbassov DD, Guertin DA, Ali SM, Sabatini DM (2005) Phosphorylation and regulation of Akt/PKB by the rictor-mTOR complex. Science 307**:** 1098-1101

Sherk AB, Frigo DE, Schnackenberg CG, Bray JD, Laping NJ, Trizna W, Hammond M, Patterson JR, Thompson SK, Kazmin D et al (2008) Development of a small-molecule serum- and glucocorticoid-regulated kinase-1 antagonist and its evaluation as a prostate cancer therapeutic. Cancer Res 68**:** 7475-7483

Sommer EM, Dry H, Cross D, Guichard S, Davies BR, Alessi DR (2013) Elevated SGK1 predicts resistance of breast cancer cells to Akt inhibitors. Biochem J 452**:** 499-508

Soukas AA, Kane EA, Carr CE, Melo JA, Ruvkun G (2009) Rictor/TORC2 regulates fat metabolism, feeding, growth, and life span in Caenorhabditis elegans. Genes Dev 23**:** 496-511

Stephens L, Anderson K, Stokoe D, Erdjument-Bromage H, Painter GF, Holmes AB, Gaffney PR, Reese CB, McCormick F, Tempst P et al (1998) Protein kinase B kinases that mediate phosphatidylinositol 3,4,5- trisphosphate-dependent activation of protein kinase B. Science 279**:** 710-714

Stokoe D, Stephens LR, Copeland T, Gaffney PR, Reese CB, Painter GF, Holmes AB, McCormick F, Hawkins PT (1997) Dual role of phosphatidylinositol-3,4,5-trisphosphate in the activation of protein kinase B. Science 277**:** 567-570

Vanhaesebroeck B, Leevers SJ, Ahmadi K, Timms J, Katso R, Driscoll PC, Woscholski R, Parker PJ, Waterfield MD (2001) Synthesis and Function of 3-Phosphorylated Inositol Lipids. Annu Rev Biochem 70**:** 535-602.

Vanhaesebroeck B, Stephens L, Hawkins P (2012) PI3K signalling: the path to discovery and understanding. Nature reviews Molecular cell biology 13**:** 195-203

Vasudevan KM, Barbie DA, Davies MA, Rabinovsky R, McNear CJ, Kim JJ, Hennessy BT, Tseng H, Pochanard P, Kim SY et al (2009) AKT-independent signaling downstream of oncogenic PIK3CA mutations in human cancer. Cancer Cell 16**:** 21-32

Virbasius JV, Song X, Pomerleau DP, Zhan Y, Zhou GW, Czech MP (2001) Activation of the Akt-related cytokine-independent survival kinase requires

interaction of its phox domain with endosomal phosphatidylinositol 3-phosphate. Proc Natl Acad Sci U S A 98**:** 12908-12913.

Wang Y, Zhou D, Chen S (2014) SGK3 is an androgen-inducible kinase promoting prostate cancer cell proliferation through activation of p70 S6 kinase and up-regulation of cyclin D1. Mol Endocrinol 28**:** 935-948

Wang Y, Zhou D, Phung S, Masri S, Smith D, Chen S (2011) SGK3 is an estrogen-inducible kinase promoting estrogen-mediated survival of breast cancer cells. Mol Endocrinol 25**:** 72-82

Wu WI, Voegtli WC, Sturgis HL, Dizon FP, Vigers GP, Brandhuber BJ (2010) Crystal structure of human AKT1 with an allosteric inhibitor reveals a new mode of kinase inhibition. PloS one 5**:** e12913

Xu J, Wan M, He Q, Bassett RL, Jr., Fu X, Chen AC, Shi F, Creighton CJ, Schiff R, Huo L et al (2012) SGK3 is associated with estrogen receptor expression in breast cancer. Breast Cancer Res Treat 134**:** 531-541

Zhang H, Zha X, Tan Y, Hornbeck PV, Mastrangelo AJ, Alessi DR, Polakiewicz RD, Comb MJ (2002) Phosphoprotein analysis using antibodies broadly reactive against phosphorylated motifs. The Journal of biological chemistry 277**:** 39379-39387.

Figure legends

FIGURE 1. Prolonged treatment with Akt inhibitors leads to upregulation of SGK3. ZR-75-1 and CAMA-1 cell lines were treated with 1 μM MK-2206 or 1 μM AZD5363, for indicated time periods. Cell lysates were subjected to (A) immunoblot analysis with the indicated antibodies or (B) mRNA isolation followed by cDNA preparation. Real-time PCR was performed on cDNA samples using specific primers against SGK1, SGK2 and SGK3 isoforms. Relative mRNA levels were calculated using 2^(-deltadelta) Ct method using DMSO treated samples as calibrator. (C) ZR-75-1 and CAMA-1 cells were treated with 1 μM MK-2206 or 1 μM AZD5363 for a total of 10 days. After 7 day treatment, SGK3 was knocked down by using three different shRNA probes, named SGK3 A, B and C and compared to a control shRNA probes, named sh scramble. Cells were maintained in the presence or absence of the indicated inhibitor during this period. At day 10 cells were lysed and subjected to immunoblot analysis with the indicated antibodies.

FIGURE 2. Prolonged treatment with Class I PI3K inhibitors leads to upregulation of SGK3. (A) The indicated cell lines were treated with either 1μM MK-2206, 1 μM AZD5363, 1μM GDC0941 or 1μM BKM120 for the indicated times. Cell lysates were subjected to immunoblot analysis with indicated antibodies. (B) The indicated cells were treated as in (A) and SGK3 was immunoprecipitated from the lysates using an anti-SGK3 antibody. The immunoprecipitates (IP) were subjected to *in vitro* kinase assay by measuring phosphorylation of the Crosstide substrate peptide in the presence of 0.1 mM ^{32}PγATP in a 30 min 30^{o}C reaction (upper panel) followed by immunoblot analysis with the indicated antibodies (lower panel). Kinase reactions are presented as means ± SD for triplicate reaction.

FIGURE 3. SGK3 activity induced by inhibition of PI3k/Akt is regulated by hVps34 and mTORC2. (A) ZR-75-1 cells were treated with 1 μM MK-2206 for 5 days and then one hour (1h) prior to cell lysis, cells were further treated with increasing doses of VPS34-IN1. Cell lysates were subjected to immunoblot analysis with indicated antibodies. (B) ZR-75-1 cells cultured in serum in the absence of Akt inhibitor were treated for one hour (1h) with the indicated concentrations of VPS34-IN1. The cell lysates were analysed by immunoblot using the indicated antibodies. (C) ZR-75-1 cells were treated for 5 days with either 1 μM MK-2206, 1 μM AZD5363, 1 μM GDC0941 or 1 μM BKM120. One hour prior to lysis the cells were incubated in the presence or absence of 1 μM VPS34-IN1. SGK3 was immunoprecipitated from lysates and subjected to *in vitro* kinase assay by measuring phosphorylation of the Crosstide substrate peptide in the presence of 0.1 mM ^{32}PγATP in a 30 min 30^{o}C reaction (upper panel). Kinase reactions are presented as means ± SD for triplicate reaction. Immunoprecipitates (IP) and lysates were analysed by immunoblot with the indicated antibodies. One-hour (1h) treatment with the PDK1 inhibitor GSK2334470 (Najafov et al, 2011) (1 μM) was used as a control for SGK3 inhibition. (D) ZR-75-1 cells were stably transfected with either a control shRNA vector (scrambled) or a shRNA vector that targets Rictor expression (shRictor). The cells were grown in the presence or absence of 1 μM MK-2206 or 1 μM

GDC0941 for 5 days. SGK3 was immunoprecipitated from the lysates and subjected to *in vitro* kinase assay as in (C). Immunoprecipitates (IP) and lysates (lower panel) were also subjected to immunoblot analysis with the indicated antibodies. (D) ZR-75-1 cells were cultured in the absence or presence of 1 μM MK-2206 for 5 days. Cells were then treated in the absence or presence of 0.1 μM AZD8055 or 0.1 μM Rapamycin for 1 hour (1h). SGK3 was immunoprecipitated and subjected to in vitro kinase assay as in (C). The immunoprecipitates (IP) and lysates were analysed with indicated antibodies.

FIGURE 4. PtdIns(3)P binding to PX domain of SGK3 promotes phosphorylation and activation by PDK1. SGK3 [S486E]-GST and SGK3 [R90A S486]-GST were purified from HEK293 cells transiently overexpressing these enzymes. One hour prior to lysis, cells were treated with 5 μM VPS34-IN1 and 5 μM GSK2334470 to ensure that the SGK3 was in its inactive dephosphorylated form. (A) SGK3[S486E]-GST was incubated with lipid vesicles comprising phosphatidylcholine (PC) and phosphatidylserine (PS) containing the indicted concentrations of PtdIns or PtdIns(3)P in the presence or absence of added recombinant PDK1 (50 ng) and kinase reactions were initiated by addition of MgATP. After 30 min at 30°C, PDK1 was inhibited by addition of the 1 μM GSK2334470 PDK1 inhibitor and reaction mixture was supplemented with 2 μg GST-NDRG1 SGK3 substrate. After another 30 min at 30°C the reaction was terminated by addition of SDS Sample Buffer. The reaction mixtures were subjected to immunoblot analysis with the indicated antibodies. (B) As in (A) except that non PtdIns(3)P-binding mutant SGK3[R90A, S486E]-GST was utilised.

FIGURE 5. 14h selectively suppresses both the activity and activation of SGK3 by PDK1 and mTORC2. (A) Chemical structure of the Sanofi-14h SGK inhibitor. (B) IC50 values of Sanofi-14h SGK inhibitor on indicated recombinant kinases. (C) Protein kinase profiling undertaken against the Dundee panel of 140 protein kinases in the presence of 1 μM Sanofi-14h at the International Centre for protein Kinase Profiling. The result for each kinase is presented as a mean kinase activity of the reaction taken in triplicate relative to a control reaction where the inhibitors were omitted. Abbreviations and assay conditions are described at http://www.kinase-screen.mrc.ac.uk. (D) ZR-75-1 cells were treated for one hour (1h) with the indicated concentrations of 14h. The cell lysates were analysed by immunoblot analysis using the indicated antibodies. (E) ZR-75-1 cells were treated for one hour (1h) with the indicated concentrations of 14h. SGK3 was immunoprecipitated from cell lysates and subjected to *in vitro* kinase assay by measuring phosphorylation of the Crosstide substrate peptide in the presence of 0.1 mM ^{32}PγATP in a 30 min 30°C reaction (upper panel). Kinase reactions are presented as means ± SD for triplicate reaction. Immunoprecipitates (IP) were also analysed by immunoblot with the indicated antibodies. (F) The effect of the indicated concentration of 14h on the ability of SGK3[S486E]-GST to be activated by PDK1 in the presence of PtdIns(3)P was assessed as described in the legend to Figure 4.

FIGURE 6. SGK3 counteracts inhibition of the PI3K-Akt pathway by phosphorylating TSC2 and stimulating S6K1. ZR-75-1 cells were treated with 1 μM MK-2206 for indicated times. SGK3 (upper panel) and S6K1 (middle panel) were immunoprecipitated and subjected to *in vitro* kinase assay by measuring phosphorylation of the Crosstide substrate peptide in the presence of 0.1 mM ^{32}PγATP in a 30 min 30^{o}C reaction. Kinase reactions are presented as means ± SD for triplicate reaction. Immunoprecipitates (IP) were also analysed by immunoblot with the indicated antibodies. The cell lysates were also analysed by immunoblot using the indicated antibodies (lower panel).

FIGURE 7. SGK3 counteracts inhibition of the PI3K-Akt pathway by phosphorylating TSC2 and stimulating mTORC1. ZR-75-1 cells were treated for 1 hour (1h) or 5 days with 1 μM MK-2206, 1 μM GDC0941 or 3 μM 14h inhibitors, alone or in combination, as indicated. (A) The cell lysates were analysed by immunoblot using the indicated antibodies. (B) SGK3 (upper panel), Akt1 (middle panel) and S6K1 (lower panel) were immunoprecipitated from the same cell lysates and subjected to *in vitro* kinase assay by measuring phosphorylation of the Crosstide substrate peptide for kinases in the presence of 0.1 mM ^{32}PγATP in a 30 min, 30^{o}C reaction. Kinase reactions are presented as means ± SD for triplicate reaction. Immunoprecipitates (IP) were also analysed by immunoblot with the indicated antibodies. (C) SGK3 was knocked down in ZR-75-1 cells by using shRNA probe B and compared to a control shRNA probe, named sh scramble. After infection, the cells were kept for 2 days in puromycin selection media and then seeded for the experiment. The cells were treated with 1 μM MK-2206 for 1 hour (1h) or 5 days. The cell lysates were subjected to immunoblot analysis with the indicated antibodies.

FIGURE 8. Dual treatment with Akt and SGK inhibitors reduces tumour growth in BT-474 xenograft model. (A) BT-474 cells were treated for the indicated times with the 0.3 μM MK-2206. The cell lysates were analysed by immunoblot using the indicated antibodies. (B) BT474c cells were treated with inhibitors as indicated either as monotherapy or in combination and cell confluency measured on the Incucyte ZOOM every 4 hours for up to 4 weeks. (C) BT-474 cells were injected subcutaneously into athymic *Foxn1^{nu}* nude mice. Mice were treated with either vehicle (8 mice) or MK-2206 (100mg/kg) (10 mice) or 14h (25mg/kg) (6 mice) or both, MK-2206 and 14h (10 mice) for 24 days. The tumour volume was measured twice a week. Tumour growth was represented as the fold change mean ± SEM. (D) All mice were weighed at the end of the treatments. Results are presented as mean ± SD. (E) Plasma concentrations of MK-2206 and 14h were analysed in samples obtained 2-3 hours after the administration of the last dose on the 24th day of treatment. Results are presented as a mean ± SD from three different samples. (F) Tumours were harvested at the end of the experiment, four hours after the last dosage and subjected to immunohistochemical analysis using cleaved Caspase 3 antibody (clCasp3) . Apoptotic sells were counted in 25 fields per each condition (left panel) and quantified as clCasp3 positive cells/field (right panel). Representative images are shown. Bar 100 μm (G) Tumours were harvested at the end of the

experiment, four hours after the last dosage and subjected to immunohistochemical analysis with the indicated antibodies. Representative images are shown. Bar 100 μm. (H) Tumours were obtain the same way as (G) and subjected to immunoblot analysis with indicated antibodies. Six different tumours were analysed from each treatment group.

FIGURE 9. Prolonged exposure to Akt or Class I PI3K inhibitors induce transcriptional changes in human kinome

ZR-75-1 cells were treated for 5 days with 1μM MK-2206 (A), 1 μM AZD5363 (B), 1μM GDC0941 (C) or DMSO. Human mRNAs were hybridised to NanoString human kinome and control code sets, then subjected to quantification using NanoString software. Results are presented as mRNA change of each kinase relative to mRNA isolated from control sample treated with DMSO. To permit data compaction, and simple kinome-wide comparisons, the fold changes are log2 transformed. The kinase mRNAs exhibiting prominent changes are annotated, with SGK3 highlighted in red. Similar profiles were obtained in one independent experiment.

Supplementary Figure legends

Supplementary Figure 1. **Prolonged treatment with Class I PI3K and Akt inhibitors leads to upregulation of SGK3 mRNA**. ZR-75-1 (left panel), CAMA-1 (middle panel) and T47D (right panel) cells were treated for 5 days with either 1 μM MK-2206, 1 μM AZD5363, 1 μM GDC0941 or 1 μM BKM120. mRNA isolation was followed by cDNA preparation. Real -time PCR was performed on cDNA samples using specific primers against SGK3 isoform. Relative mRNA levels were calculated using 2^(-deltadelta) Ct method using DMSO treated samples as calibrator.

Supplementary Figure 2. **Further evidence that SGK3 activity induced by inhibition of PI3k/Akt is regulated by hVps34**. (A) ZR-75-1 cells were treated with 1 μM MK-2206 for 5 days and then one hour (1h) prior to cell lysis cells were further treated with increasing doses of SAR405. (B) ZR-75-1 cells cultured in serum in the absence of Akt inhibitor were treated for one hour (1h) with the indicated concentrations of SAR405. The cell lysates were analyzed by immunoblot using the indicated antibodies. (C) ZR-75-1 cells were treated for 5 days with 1 μM MK-2206 or 1 μM GDC0941. One hour prior to lysis the cells were incubated in the presence of absence of 0.3 μM SAR405. SGK3 was immunoprecipitated from lysates and subjected to i*n vitro* kinase assay by measuring phosphorylation of the Crosstide substrate peptide in the presence of 0.1 mM 32PγATP in a 30 min 30 ^{o}C reaction (upper panel). Kinase reactions are presented as means ± SD for triplicate reaction. Immunoprecipitates (IP) and lysates were also analysed by immunoblot with the indicated antibodies.

Supplementary Figure 3. Structure and IC50 data for 14g, 14i and 14n SGK inhibitors. (A) Chemical structures of Sanofi-14g, -14i and -14n compounds. (B) IC50 values of inhibitors on indicated recombinant kinases.

Supplementary Figure 4. Protein kinase profiling of 14g, 14i and 14n SGK inhibitors. Profiling of Sanofi 14g (A), 14i (B) and 14n (C) compounds was undertaken against the Dundee panel of 140 protein kinases in the presence of 1 μM compound at the International Centre for protein Kinase Profiling. The result for each kinase is presented as a mean kinase activity of the reaction taken in triplicate relative to a control reaction where the inhibitors were omitted. Abbreviations and assay conditions are described at http://www.kinase-screen.mrc.ac.uk.

Supplementary Figure 5. SGK3 inhibition does not ablate residual mTORC1 activity during short term inhibitor treatment. ZR-75-1 cells were treated for 1 hour (1h) with 1 μM MK-2206, 1 μM GDC0941 or 3 μM 14h inhibitors, alone or in combination, as indicated. The cell lysates were analysed by immunoblot using the indicated antibodies.

Supplementary Figure 6. hVps34 inhibition exerts the similar effect as SGK3 inhibition in regulation of TSC2-mTORC1 axis. ZR-75-1 cells were treated for 1 hour (1h) or 5 days with 1 μM MK-2206, 1 μM GDC0941 or 1 μM

VPS34-IN1 inhibitors, alone or in combination, as indicated. The cell lysates were analysed by immunoblot using the indicated antibodies.

Supplementary Figure 7. SGK3 phosphorylate a subset of proteins with RxRxxS/T motif upon sustained inhibition with Class I PI3K or Akt inhibitors. ZR-75-1 cells were treated for 1 hour (1h) or 5 days with 1 μM MK-2206, 1 μM GDC0941 or 3 μM 14h inhibitors, alone or in combination, as indicated. The cell lysates were analysed by immunoblot using the antibody against phosphorylated Akt phosphorylation consensus motif (RxRxxpS/pT). Red asterisk indicates potential dual Akt and SGK3 substrates whose phosphorylation is induced following 5 day MK-2206 or GDC0941 treatment and suppressed by a subsequent 1-hour treatment with 14h. Blue circles indicates potential Akt selective substrates whose phosphorylation is inhibited by MK-2206 or GDC0941 treatment and but do not become re-phosphorylated following 5 day incubation with these inhibitors under conditions where SGK3 is upregulated.

Supplementary Figure 8. Akt inhibition induces dose dependent inhibition of cell growth in BT-474c cells *in vitro.* BT-474c cells were treated with DMSO, 3 μM 14h, and indicated doses of MK-2206 (A) or AZD5363 (B) inhibitors. Cell confluency was measured on the Incucyte ZOOM every 4 hours for up to 6 days.

Supplementary Figure 9. SGK3 counteracts inhibition of the PI3K-Akt pathway by phosphorylating TSC2 and stimulating mTORC1 in BT-474c cells. BT-474c cells were treated for 1 hour (1h) or 5 days with 1 μM MK-2206 or 3 μM 14h, as indicated. SGK3 (upper panel) and S6K1 (middle panel) were immunoprecipitated and subjected to *in vitro* kinase assay by measuring phosphorylation of the Crosstide substrate peptide in the presence of 0.1 mM ^{32}PγATP in a 30 min 30^{o}C reaction. Kinase reactions are presented as means ± SD for triplicate reaction. Immunoprecipitates (IP) were also analysed by immunoblot with the indicated antibodies. The cell lysates were subjected to immunoblot analysis using the indicated antibodies (bottom panel).

Supplementary Figure 10. Total human AGC kinase mRNA expression profiles in cells exposed to compounds for 2 days.
ZR-75-1 cells were grown in the presence or absence of DMSO, 1 μM MK-2206, 1 μM AZD5363 or 1 μM GDC0941 for 2 days, and total human AGC kinase mRNA levels were quantified using NanoString software. Data are presented as log10 values of triplicate data ± SD. The rank order position of SGK3 mRNA in each condition, and its relative expression towards all human AGC kinases, is annotated in red (left panel). All AGC kinase mRNAs exhibiting a ≥2-fold change in expression level in the appropriate compound relative to DMSO control are quantified (right panel). *=p<0.05, **=p<0.01, ***=p<0.001 (right panel).

Supplementary Figure 11. Total human AGC kinase mRNA expression profiles in cells exposed to compounds for 5 days.
ZR-75-1 cells were grown in the presence or absence of DMSO, 1 μM MK-2206, 1 μM AZD5363 or 1 μM GDC0941 for 5 days, and total human AGC kinase mRNA levels were quantified using NanoString software. Data are presented as log10

values of triplicate data ± SD. The rank order position of SGK3 mRNA in each condition, and its relative expression towards all human AGC kinases, is annotated in red (left panel). All AGC kinase mRNAs exhibiting a ≥2-fold change in expression level in the appropriate compound relative to DMSO control are quantified (right panel). *=p<0.05, **=p<0.01 (right panel).

Excel File 1. Normalised whole kinome mRNA counts from ZR-75-1 cells treated with DMSO, 1 μM MK-2206, 1 μM AZD5363 or 1 μM GDC0941 for 5 days.

Supplementary Tables 1-4.
Results are presented as the percentage of kinase activity in DMSO control reactions. Protein kinases were assayed *in vitro* in the presence of 1μM Sanofi-14g (Table 1), -14h (Table 2), -14i (Table 3) and -14n (Table 4) compounds, as described on the International Centre for Kinase Profiling website (http://www.kinase-screen.mrc.ac.uk/), and the results are means ± S.D. for triplicate reactions. Abbreviations are as follows: ABL, Abelson tyrosine-protein kinase 1; AMPK, AMP-activated protein kinase; ASK, apoptosis signal-regulating kinase; BRK, breast tumour kinase; BRSK, brain-specific kinase; BTK, Bruton's tyrosine kinase; CaMK, calmodulin-dependent kinase; CaMKK, CaMK kinase; CDK, cyclin-dependent kinase; CHK, checkpoint kinase; CK, casein kinase; CLK, CDC-like kinase; CSK, C-terminal Src kinase; DAPK, death-associated protein kinase; DDR, discoidin domain receptor; DYRK, dual-specificity tyrosine-phosphorylated and regulated kinase; EF2K, elongation-factor-2 kinase; EIF2AK, eukaryotic translation initiation factor 2-alpha kinase; EPH, ephrin; ERK, extracellular signal-regulated kinase; FGF-R, fibroblast growth factor receptor; GCK, germinal centre kinase; GSK, glycogen synthase kinase; HER, human epidermal growth factor receptor; HIPK, homeodomain-interacting protein kinase; IGF1R, IGF1 receptor; IKK, inhibitory κB kinase; IR, insulin receptor; IRAK, interleukin-1 receptor-associated kinase; IRR, insulin-related receptor; JAK, Janus kinase; JNK, c-Jun N-terminal kinase; Lck, lymphocyte cell-specific protein tyrosine kinase; LKB1, liver kinase B1; MAPK, mitogen-activated protein kinase; MAPKAP-K, MAPK-activated protein kinase; MARK, microtubule-affinity regulating kinase; MEKK, MAP kinase kinase kinase; MELK, maternal embryonic leucinezipper kinase; MINK, misshapen/NIK-related kinase; MKK, MAPK kinase; MLK, mixed lineage kinase; MNK, MAPK-integrating protein kinase; MPSK, myristoylated and palmitoylated serine/threonine-protein kinase; MSK, mitogen- and stress-activated protein kinase; MST, mammalian homologue Ste20-like kinase; NEK, NIMA (never in mitosis in *Aspergillus nidulans*)-related kinase; NUAK, novel (NUA) family SnF1-like kinase; OSR, oxidative stress-responsive kinase; PAK, p21-activated protein kinase; PDGFRA, platelet-derived growth factor receptor-α; PDK, phosphoinositide-dependent kinase; PHK, phosphorylase kinase; PIM, provirus integration site for Moloney murine leukaemia virus; PINK (insect homologue), PTEN-induced kinase; PKA, cAMP-dependent protein kinase; PKB, protein kinase B; PKC, protein kinase C; PKD, protein kinase D; PLK, polo-like kinase; PRAK, p38-regulated activated kinase; PRK, protein kinase C-related kinase; RIPK, receptor-interacting protein kinase; ROCK, Rho-dependent protein kinase; RSK, ribosomal S6 kinase; S6K1, p70 ribosomal S6 kinase; SGK, serum- and glucocorticoid-induced protein kinase; SIK, salt-induced kinase; smMLCK, smooth muscle myosin light-chain kinase;

SRPK, serine/arginine protein kinase; STK, serine/threonine kinase; SYK, spleen tyrosine kinase; TAK, TGFβ-activated kinase; TAO, thousand and one amino acid; TBK1, TANK-binding kinase 1; TESK, testis-specific protein kinase; TGFBR, TGFβ receptor; TIE, tyrosine-protein kinase receptor; TLK, tousled-like kinase; TrkA, tropomyocin receptor kinase; TSSK, testis-specific serine/threonine-protein kinase; TTBK, tau-tubulin kinase; ULK, Unc-51-like kinase; VEGFR, vascular endothelial growth factor receptor; WNK, with no lysine; YES1, Yamaguchi sarcoma viral oncogene homologue 1; ZAP, ζ-chain-associated protein.

FIGURE 1.

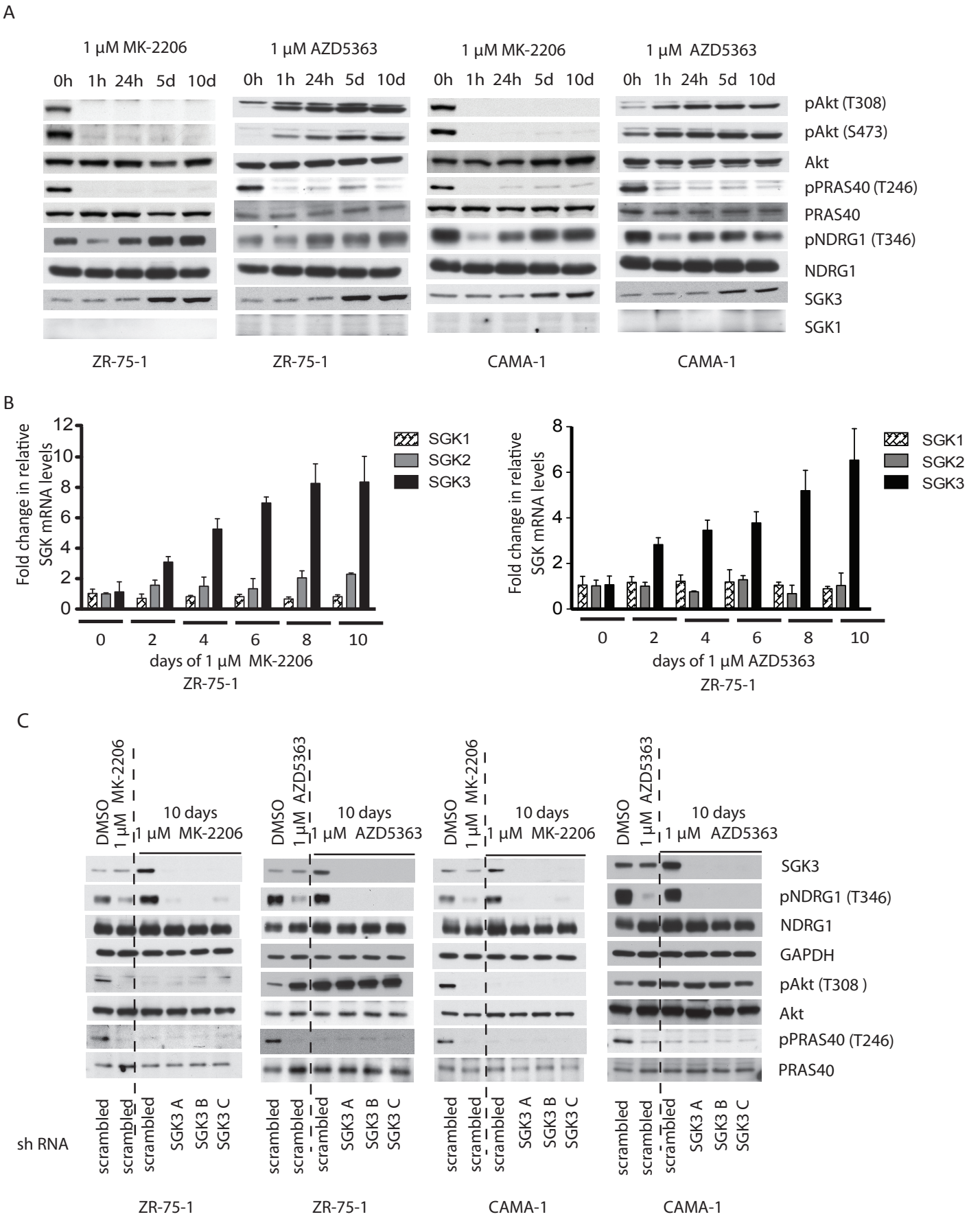
A
1 μM MK-2206
1 μM AZD5363
1 μM MK-2206
1 μM AZD5363
0h 1h 24h 5d 10d
pAkt (T308)
pAkt (S473)
Akt
pPRAS40 (T246)
PRAS40
pNDRG1 (T346)
NDRG1
SGK3
SGK1
ZR-75-1
ZR-75-1
CAMA-1
CAMA-1
B
Fold change in relative SGK mRNA levels
SGK1
SGK2
SGK3
days of 1 μM MK-2206
ZR-75-1
days of 1 μM AZD5363
ZR-75-1
C
DMSO
1 μM MK-2206
10 days 1 μM MK-2206
DMSO
1 μM AZD5363
10 days 1 μM AZD5363
SGK3
pNDRG1 (T346)
NDRG1
GAPDH
pAkt (T308)
Akt
pPRAS40 (T246)
PRAS40
sh RNA
scrambled
SGK3 A
SGK3 B
SGK3 C
ZR-75-1
ZR-75-1
CAMA-1
CAMA-1

FIGURE 2

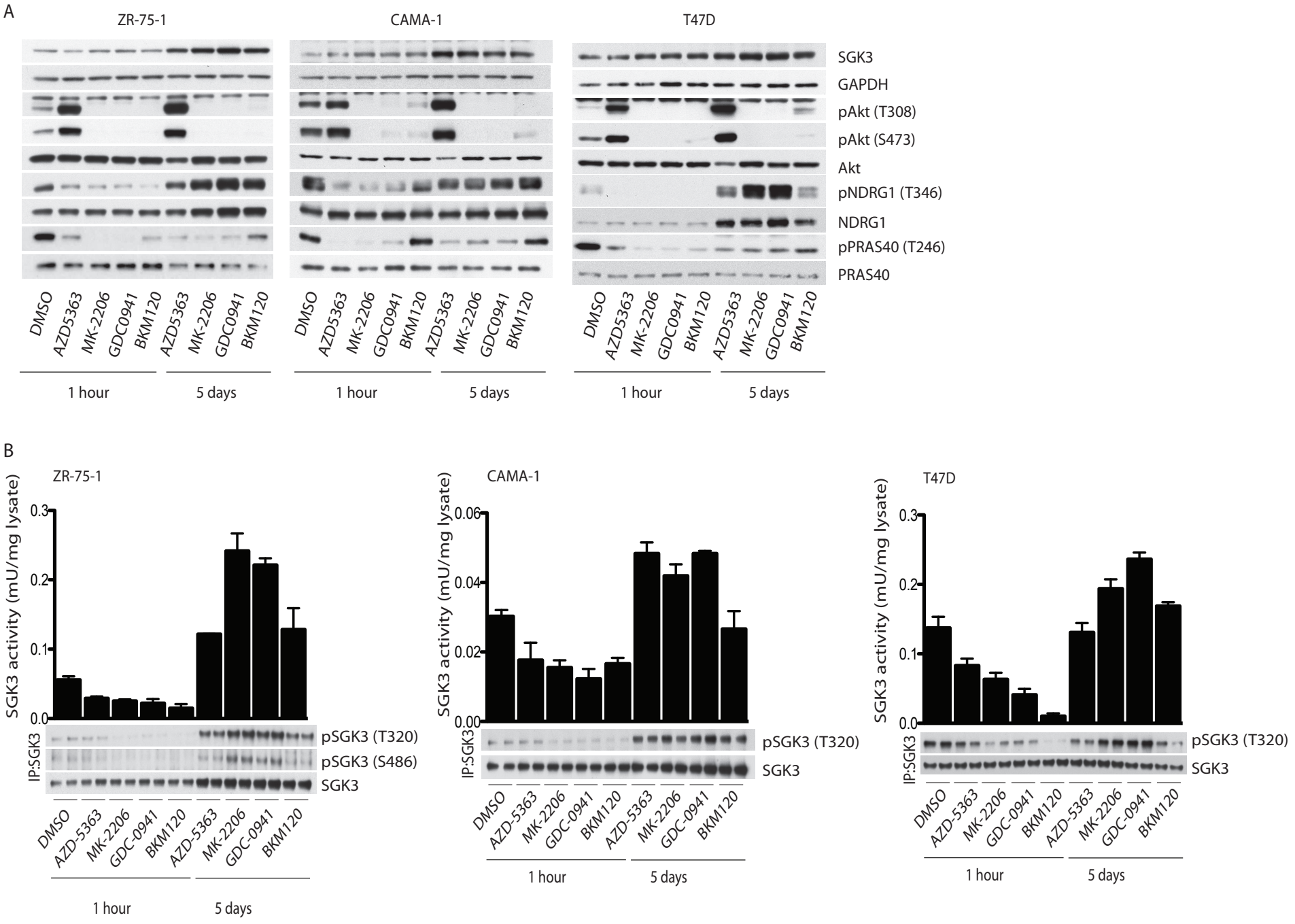
A
ZR-75-1
CAMA-1
T47D
SGK3
GAPDH
pAkt (T308)
pAkt (S473)
Akt
pNDRG1 (T346)
NDRG1
pPRAS40 (T246)
PRAS40
DMSO
AZD5363
MK-2206
GDC0941
BKM120
1 hour
5 days
B
ZR-75-1
CAMA-1
T47D
SGK3 activity (mU/mg lysate)
IP:SGK3
pSGK3 (T320)
pSGK3 (S486)
SGK3
DMSO
AZD-5363
MK-2206
GDC-0941
BKM120
1 hour
5 days

FIGURE 3

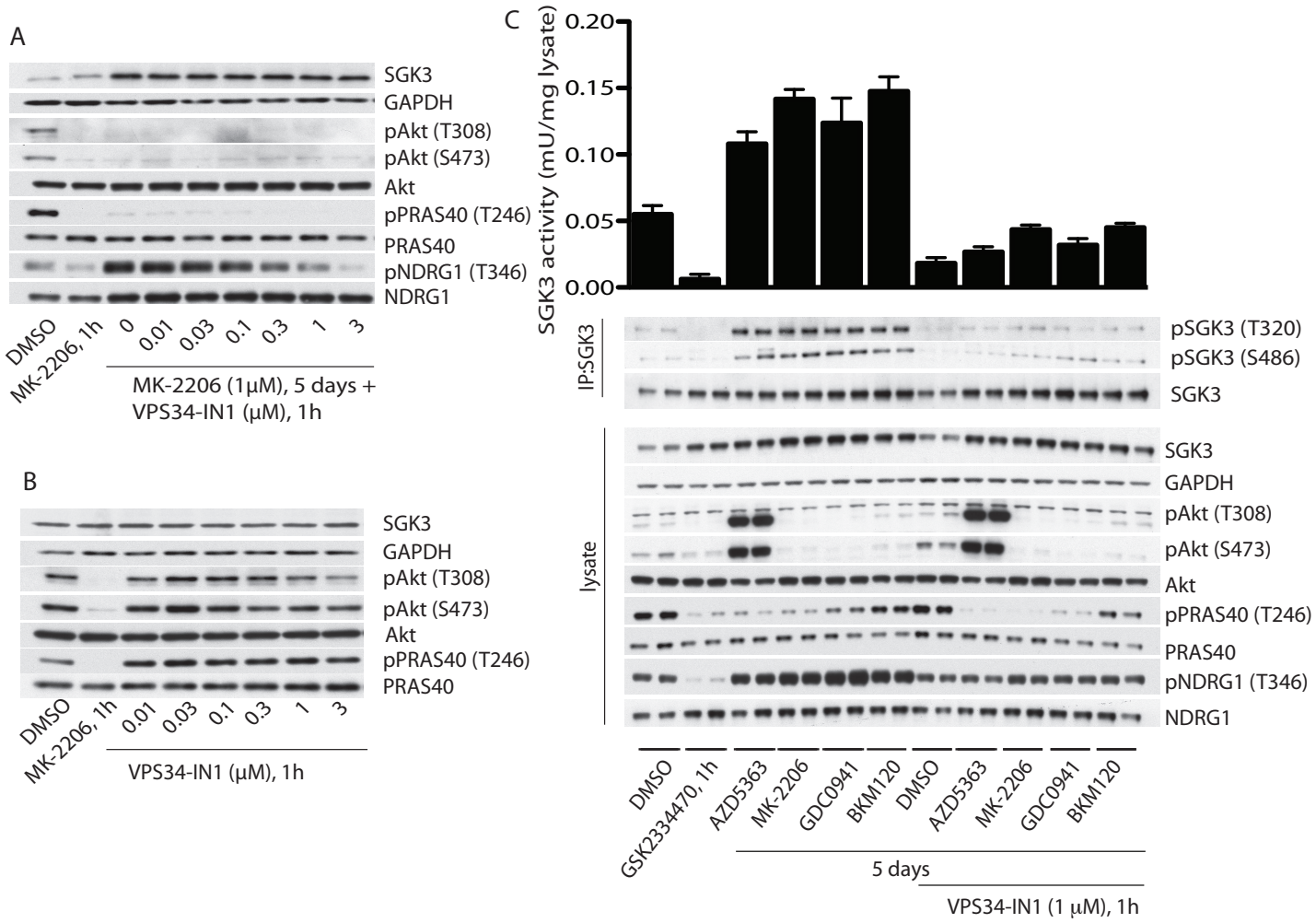
A
SGK3
GAPDH
pAkt (T308)
pAkt (S473)
Akt
pPRAS40 (T246)
PRAS40
pNDRG1 (T346)
NDRG1
DMSO
MK-2206, 1h
0
0.01
0.03
0.1
0.3
1
3
MK-2206 (1μM), 5 days +
VPS34-IN1 (μM), 1h
B
SGK3
GAPDH
pAkt (T308)
pAkt (S473)
Akt
pPRAS40 (T246)
PRAS40
DMSO
MK-2206, 1h
0.01
0.03
0.1
0.3
1
3
VPS34-IN1 (μM), 1h
C
SGK3 activity (mU/mg lysate)
0.20
0.15
0.10
0.05
0.00
IP:SGK3
pSGK3 (T320)
pSGK3 (S486)
SGK3
lysate
SGK3
GAPDH
pAkt (T308)
pAkt (S473)
Akt
pPRAS40 (T246)
PRAS40
pNDRG1 (T346)
NDRG1
DMSO
GSK2334470, 1h
AZD5363
MK-2206
GDC0941
BKM120
DMSO
AZD5363
MK-2206
GDC0941
BKM120
5 days
VPS34-IN1 (1 μM), 1h

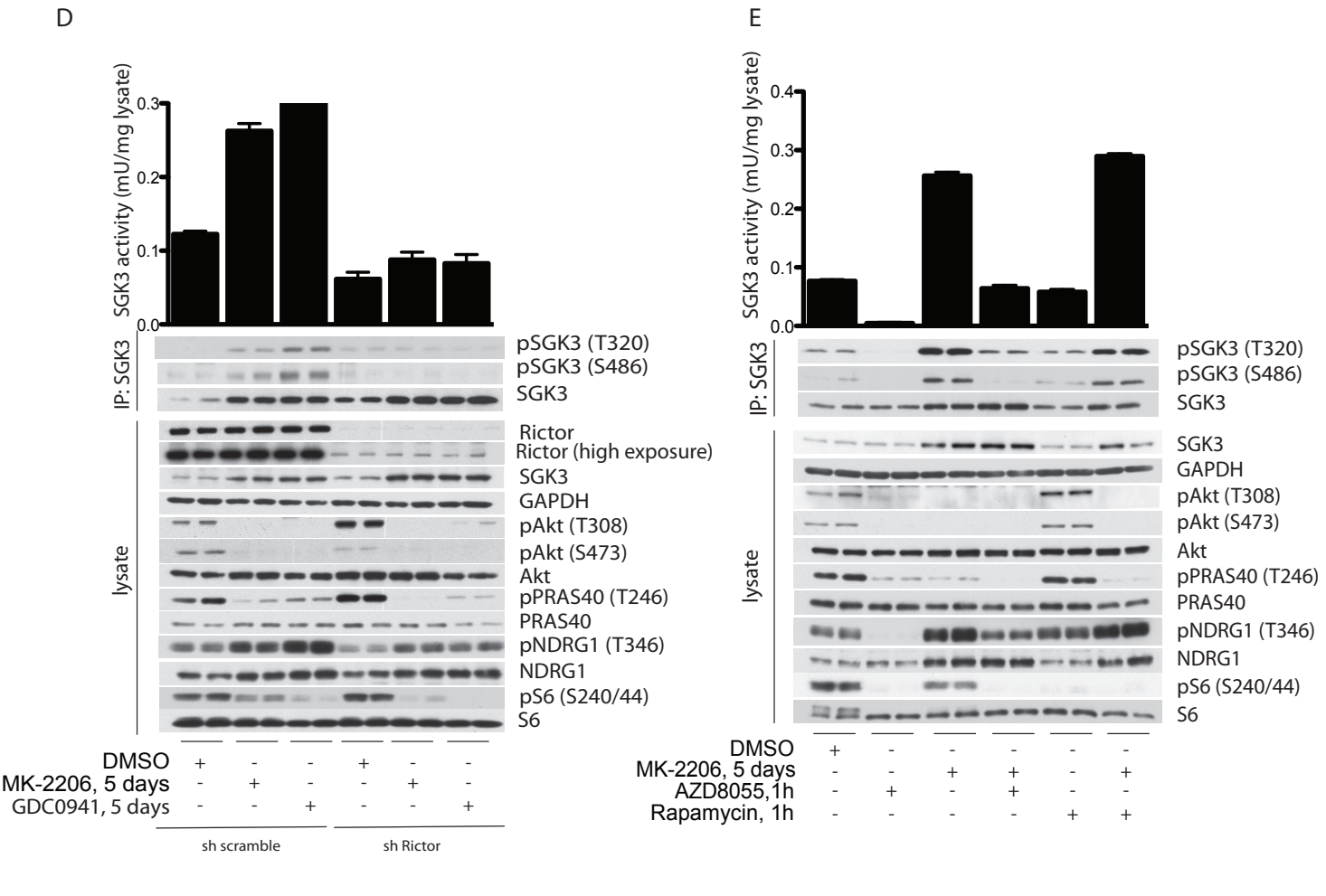
D
SGK3 activity (mU/mg lysate)
0.3
0.2
0.1
0.0
IP: SGK3
pSGK3 (T320)
pSGK3 (S486)
SGK3
lysate
Rictor
Rictor (high exposure)
SGK3
GAPDH
pAkt (T308)
pAkt (S473)
Akt
pPRAS40 (T246)
PRAS40
pNDRG1 (T346)
NDRG1
pS6 (S240/44)
S6
DMSO + - - + - -
MK-2206, 5 days - + - - + -
GDC0941, 5 days - - + - - +
sh scramble
sh Rictor
E
SGK3 activity (mU/mg lysate)
0.4
0.3
0.2
0.1
0.0
IP: SGK3
pSGK3 (T320)
pSGK3 (S486)
SGK3
lysate
SGK3
GAPDH
pAkt (T308)
pAkt (S473)
Akt
pPRAS40 (T246)
PRAS40
pNDRG1 (T346)
NDRG1
pS6 (S240/44)
S6
DMSO + - - - - -
MK-2206, 5 days - - + + - +
AZD8055,1h - + - + - -
Rapamycin, 1h - - - - + +

FIGURE 4

A

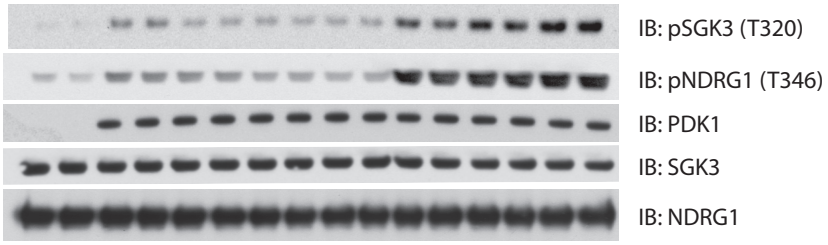

PtdIns (μM)	-	-	1	3	10	-	-	-
PtdIns(3)P (μM)	-	-	-	-	-	1	3	10
PS/PC (100 μM)	+	+	+	+	+	+	+	+
GST-PDK1 (1.6 mU/50 ng)	-	+	+	+	+	+	+	+
SGK3 S486E-GST (50 ng)	+	+	+	+	+	+	+	+
GST-NDRG1 (2 μg)	+	+	+	+	+	+	+	+

B

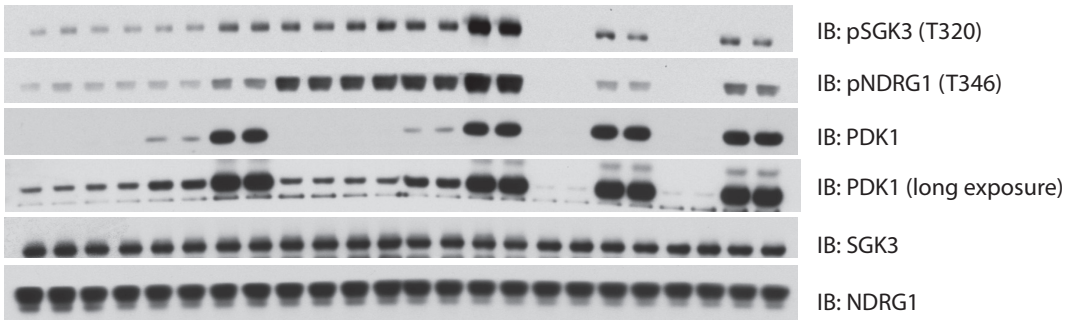

PtdIns (10 μM)	+	+	+	+	-	-	-	-	+	+	-	-
PtdIns(3)P (10 μM)	-	-	-	-	+	+	+	+	-	-	+	+
PS/PC (100 μM)	+	+	+	+	+	+	+	+	+	+	+	+
GST-PDK1 (ng)	-	0.5	5	50	-	0.5	5	50	-	50	-	50
GST-NDRG1 (2 μg)	+	+	+	+	+	+	+	+	+	+	+	+

FIGURE 5

A.

14h

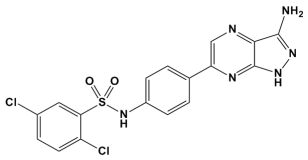

B.

kinase	14h
SGK1	0.010
SGK3	0.004
MLK1	0.215
MLK3	0.084
PKBa	>10
p70S6K	0.076

C Sanofi--14h(1μM)

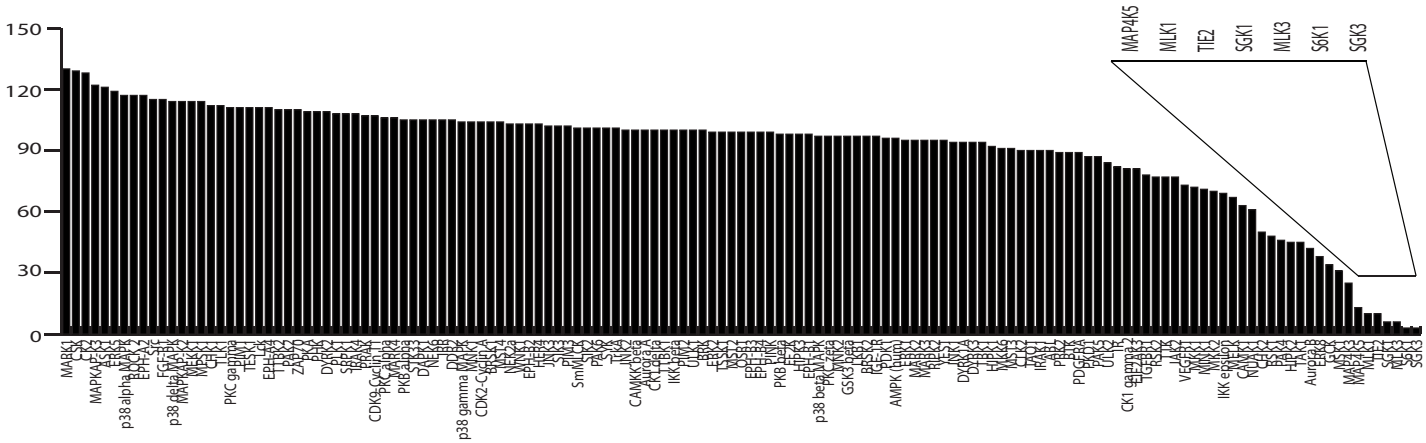

D

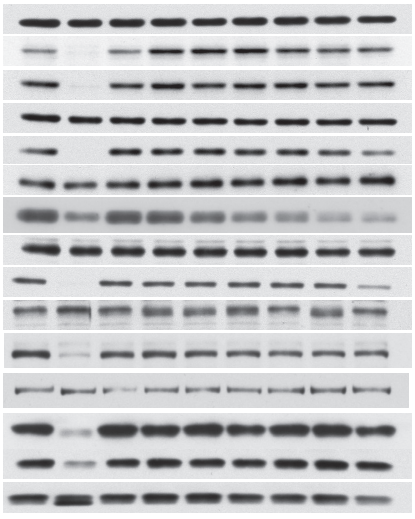

E

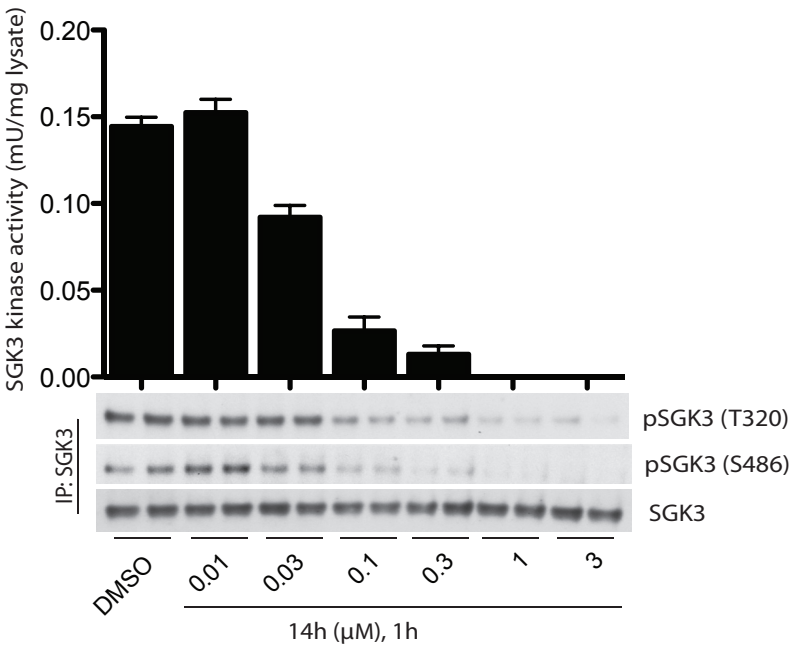

F

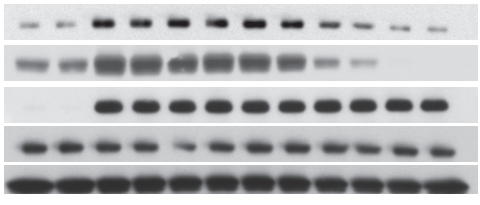

-14h (μM)	-	-	0.001	0.01	0.1	1
GST-PDK1 (1.6 mU/50 ng)	-	+	+	+	+	+
SGK3 S486E-GST (50 ng)	+	+	+	+	+	+
GST-NDRG1 (2 μg)	+	+	+	+	+	+

FIGURE 6

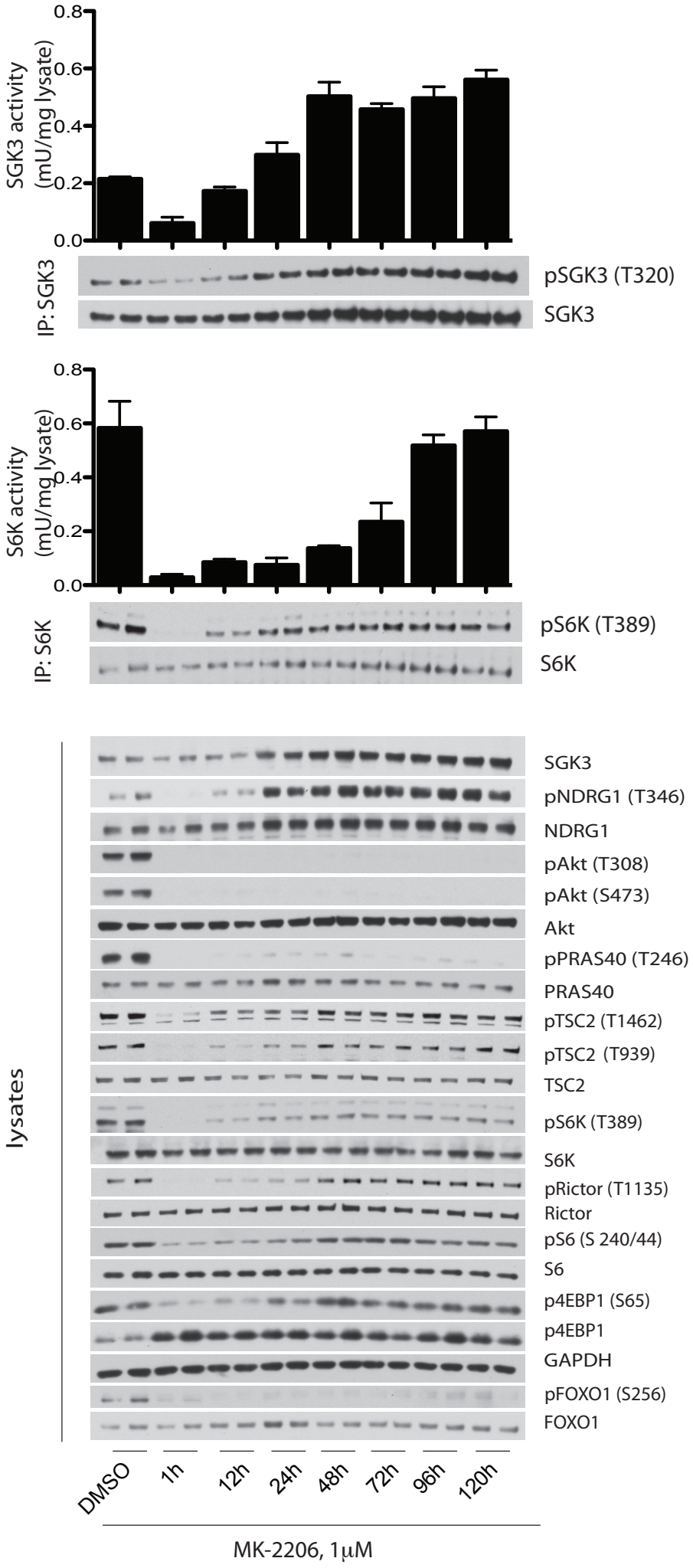
SGK3 activity (mU/mg lysate)
0.8
0.6
0.4
0.2
0.0
IP: SGK3
pSGK3 (T320)
SGK3
S6K activity (mU/mg lysate)
0.8
0.6
0.4
0.2
0.0
IP: S6K
pS6K (T389)
S6K
lysates
SGK3
pNDRG1 (T346)
NDRG1
pAkt (T308)
pAkt (S473)
Akt
pPRAS40 (T246)
PRAS40
pTSC2 (T1462)
pTSC2 (T939)
TSC2
pS6K (T389)
S6K
pRictor (T1135)
Rictor
pS6 (S 240/44)
S6
p4EBP1 (S65)
p4EBP1
GAPDH
pFOXO1 (S256)
FOXO1
DMSO
1h
12h
24h
48h
72h
96h
120h
MK-2206, 1μM

FIGURE 7

A

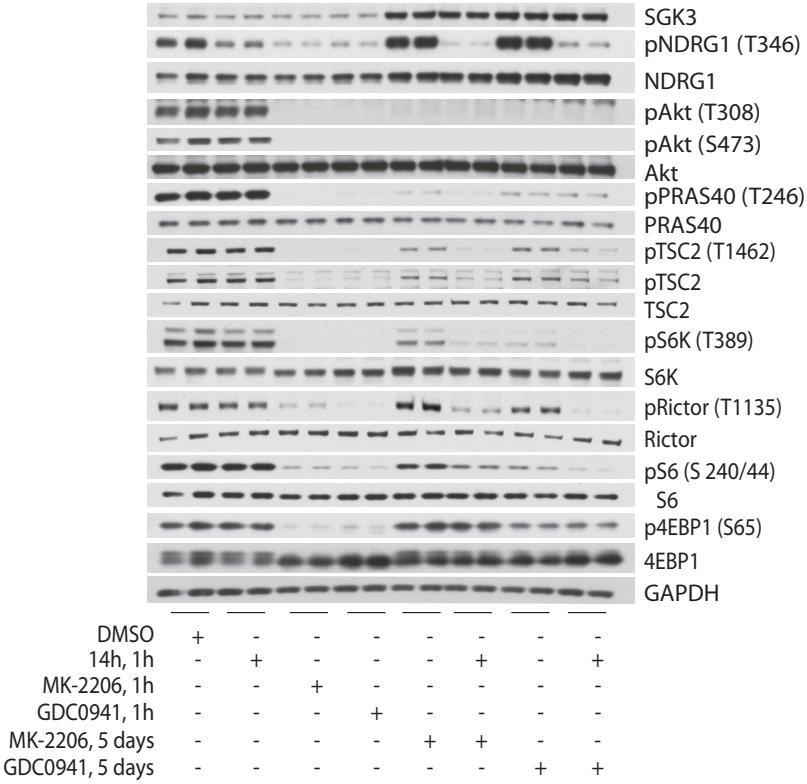
SGK3
pNDRG1 (T346)
NDRG1
pAkt (T308)
pAkt (S473)
Akt
pPRAS40 (T246)
PRAS40
pTSC2 (T1462)
pTSC2
TSC2
pS6K (T389)
S6K
pRictor (T1135)
Rictor
pS6 (S 240/44)
S6
p4EBP1 (S65)
4EBP1
GAPDH
DMSO + - - - - - - -
14h, 1h - + - - - + - +
MK-2206, 1h - - + - - - - -
GDC0941, 1h - - - + - - - -
MK-2206, 5 days - - - - + + - -
GDC0941, 5 days - - - - - - + +

B

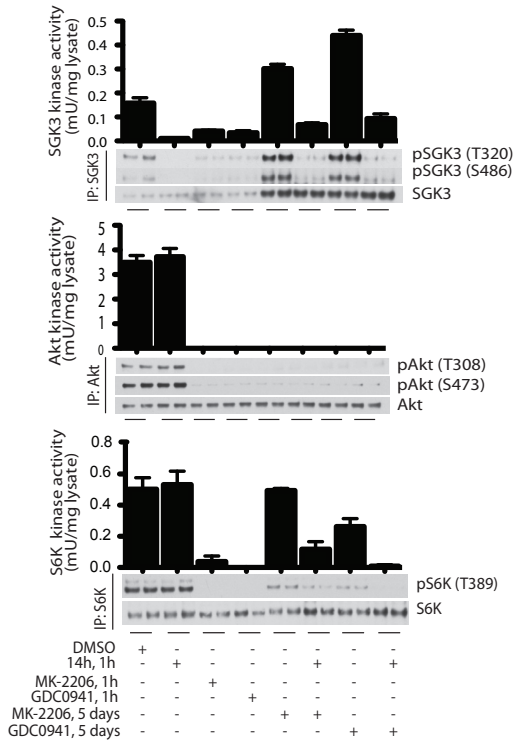
SGK3 kinase activity (mU/mg lysate)
0.5
0.4
0.3
0.2
0.1
0.0
IP: SGK3
pSGK3 (T320)
pSGK3 (S486)
SGK3
Akt kinase activity (mU/mg lysate)
5
4
3
2
1
0
IP: Akt
pAkt (T308)
pAkt (S473)
Akt
S6K kinase activity (mU/mg lysate)
0.8
0.6
0.4
0.2
0.0
IP: S6K
pS6K (T389)
S6K
DMSO + - - - - - - -
14h, 1h - + - - - + - +
MK-2206, 1h - - + - - - - -
GDC0941, 1h - - - + - - - -
MK-2206, 5 days - - - - + + - -
GDC0941, 5 days - - - - - - + +

C

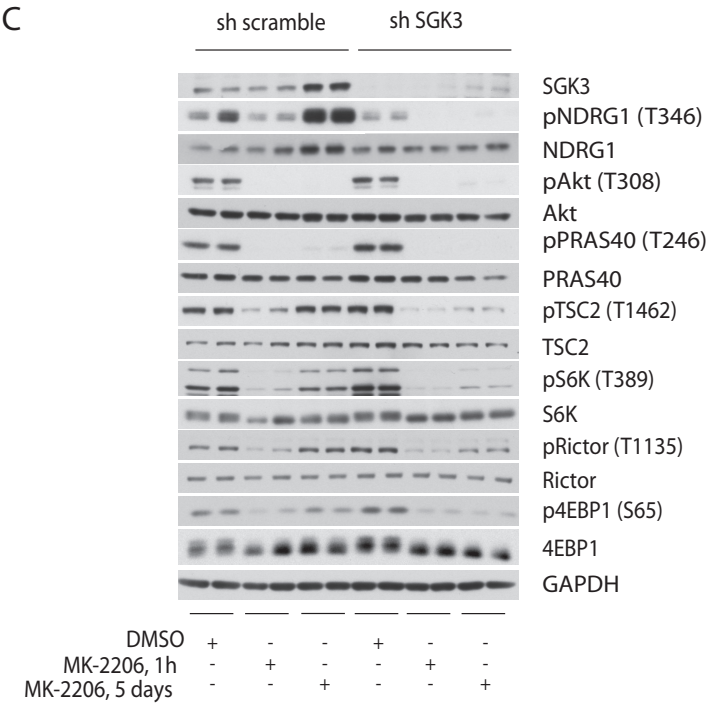
sh scramble
sh SGK3
SGK3
pNDRG1 (T346)
NDRG1
pAkt (T308)
Akt
pPRAS40 (T246)
PRAS40
pTSC2 (T1462)
TSC2
pS6K (T389)
S6K
pRictor (T1135)
Rictor
p4EBP1 (S65)
4EBP1
GAPDH
DMSO + - - + - -
MK-2206, 1h - + - - + -
MK-2206, 5 days - - + - - +

FIGURE 8

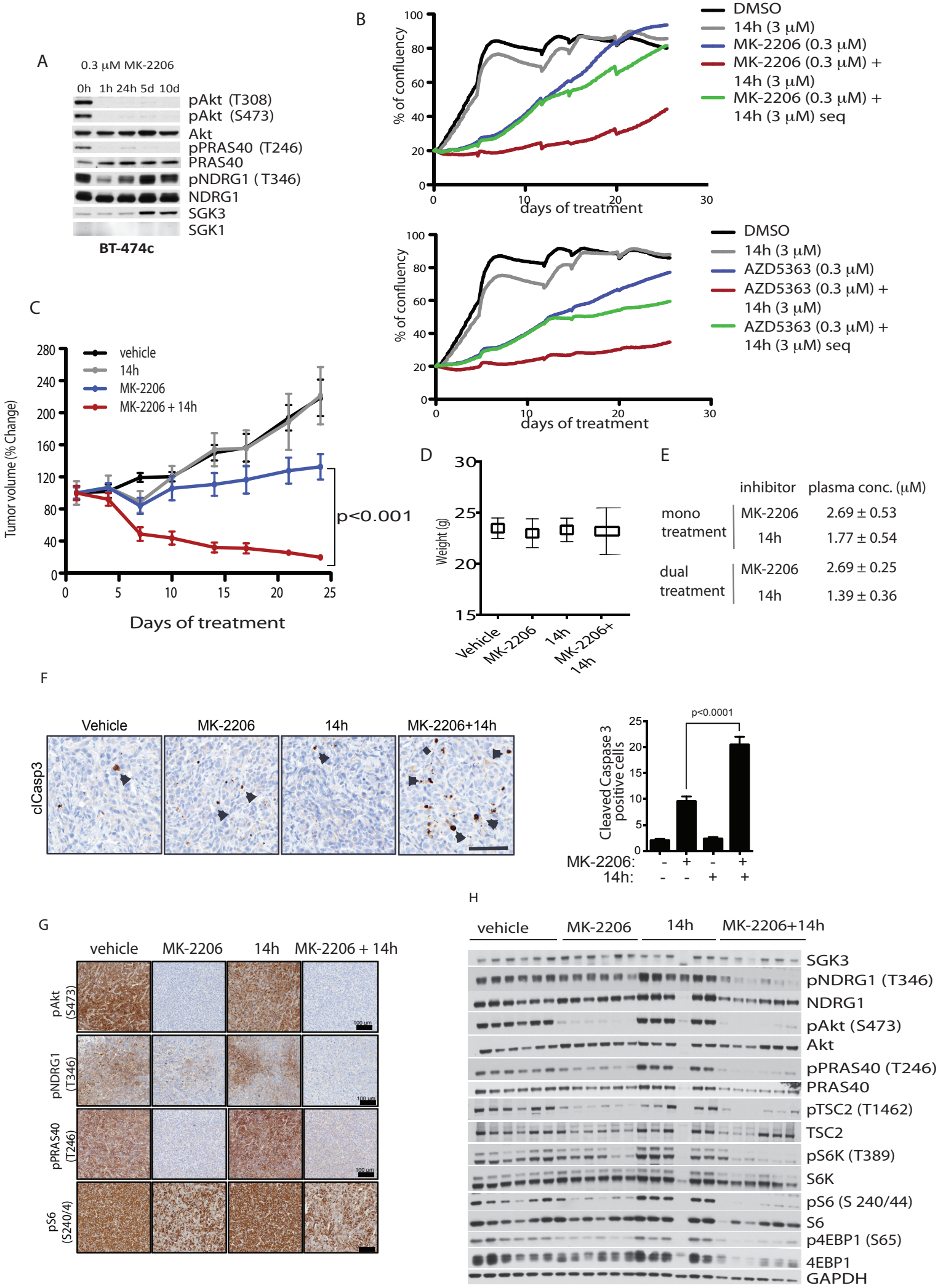
A
0.3 μM MK-2206
0h 1h 24h 5d 10d
pAkt (T308)
pAkt (S473)
Akt
pPRAS40 (T246)
PRAS40
pNDRG1 (T346)
NDRG1
SGK3
SGK1
BT-474c
B
% of confluency
days of treatment
DMSO
14h (3 μM)
MK-2206 (0.3 μM)
MK-2206 (0.3 μM) + 14h (3 μM)
MK-2206 (0.3 μM) + 14h (3 μM) seq
AZD5363 (0.3 μM)
AZD5363 (0.3 μM) + 14h (3 μM)
AZD5363 (0.3 μM) + 14h (3 μM) seq
C
Tumor volume (% Change)
Days of treatment
vehicle
14h
MK-2206
MK-2206 + 14h
p<0.001
D
Weight (g)
Vehicle
MK-2206
14h
MK-2206+ 14h
E
inhibitor
plasma conc. (μM)
mono treatment
MK-2206
2.69 ± 0.53
14h
1.77 ± 0.54
dual treatment
MK-2206
2.69 ± 0.25
14h
1.39 ± 0.36
F
Vehicle
MK-2206
14h
MK-2206+14h
cICasp3
p<0.0001
Cleaved Caspase 3 positive cells
MK-2206:
14h:
G
vehicle
MK-2206
14h
MK-2206 + 14h
pAkt (S473)
pNDRG1 (T346)
pPRAS40 (T246)
pS6 (S240/4)
H
vehicle
MK-2206
14h
MK-2206+14h
SGK3
pNDRG1 (T346)
NDRG1
pAkt (S473)
Akt
pPRAS40 (T246)
PRAS40
pTSC2 (T1462)
TSC2
pS6K (T389)
S6K
pS6 (S 240/44)
S6
p4EBP1 (S65)
4EBP1
GAPDH

FIGURE 9

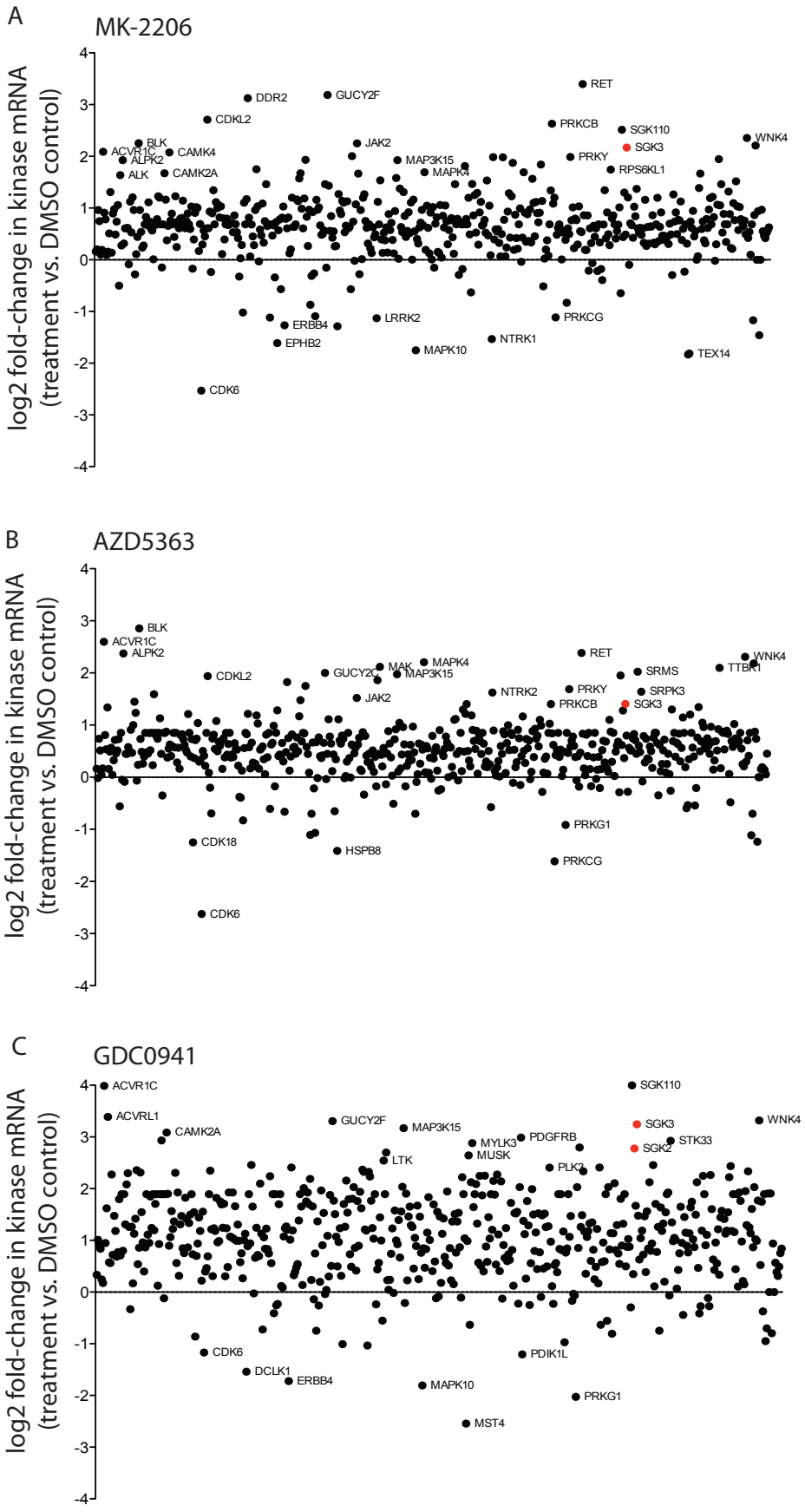
A
MK-2206
log2 fold-change in kinase mRNA
(treatment vs. DMSO control)
4
3
2
1
0
-1
-2
-3
-4
DDR2
GUCY2F
RET
CDKL2
PRKCB
SGK110
WNK4
BLK
JAK2
SGK3
ACVR1C
CAMK4
MAP3K15
PRKY
ALPK2
MAPK4
RPS6KL1
ALK
CAMK2A
ERBB4
LRRK2
PRKCG
EPHB2
MAPK10
NTRK1
TEX14
CDK6
B
AZD5363
log2 fold-change in kinase mRNA
(treatment vs. DMSO control)
BLK
ACVR1C
ALPK2
RET
WNK4
CDKL2
GUCY2C
MAK
MAPK4
SRMS
TTBK1
MAP3K15
NTRK2
PRKY
SRPK3
JAK2
PRKCB
SGK3
PRKG1
CDK18
HSPB8
PRKCG
CDK6
C
GDC0941
log2 fold-change in kinase mRNA
(treatment vs. DMSO control)
ACVR1C
SGK110
ACVRL1
GUCY2F
MAP3K15
SGK3
WNK4
CAMK2A
MYLK3
PDGFRB
STK33
SGK2
LTK
MUSK
PLK2
CDK6
PDIK1L
DCLK1
ERBB4
MAPK10
PRKG1
MST4

Supplementary FIGURE 1.

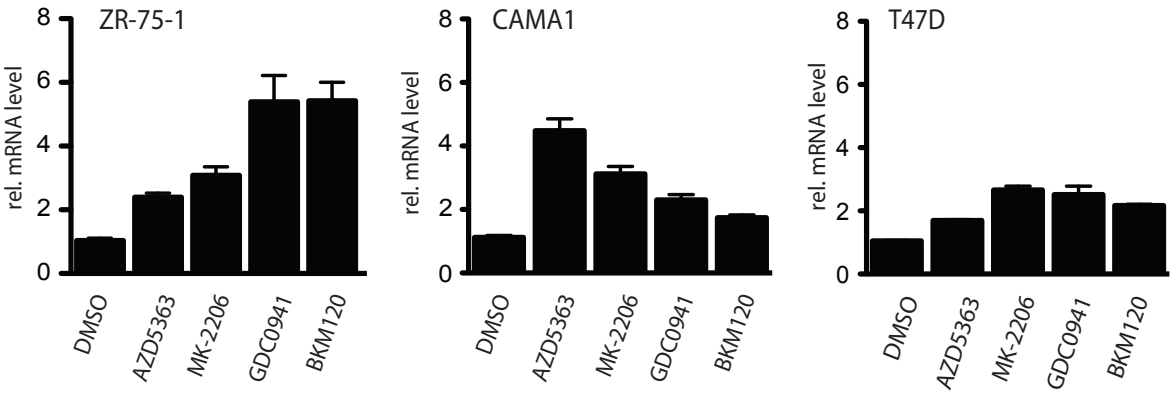

Supplementary Fig. 2

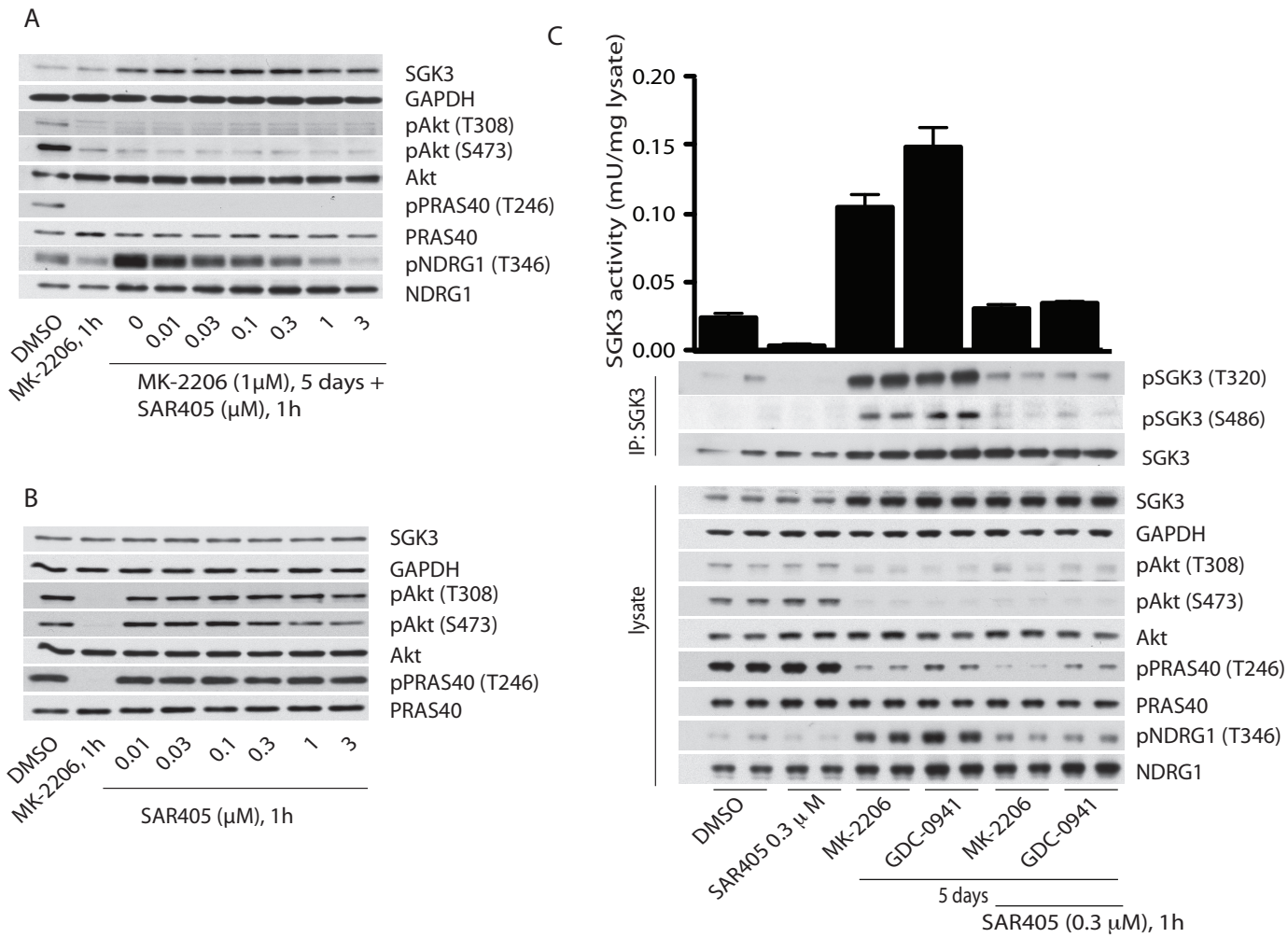

Supplementary Figure 3.

A

14g

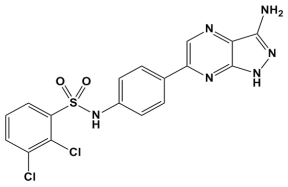

14i

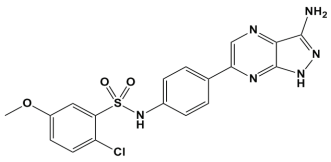

14n

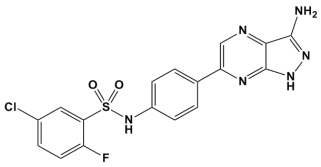

B.

kinase	14g	14i	14n
SGK1	0.05	0.07	0.013
SGK3	0.08	0.03	0.013
MLK1	0.38	0.6	0.169
MLK3	0.14	0.27	0.094
PKBa	>10	>10	>10
S6K1	0.06	0.18	0.076

Supplementary Figure 4.

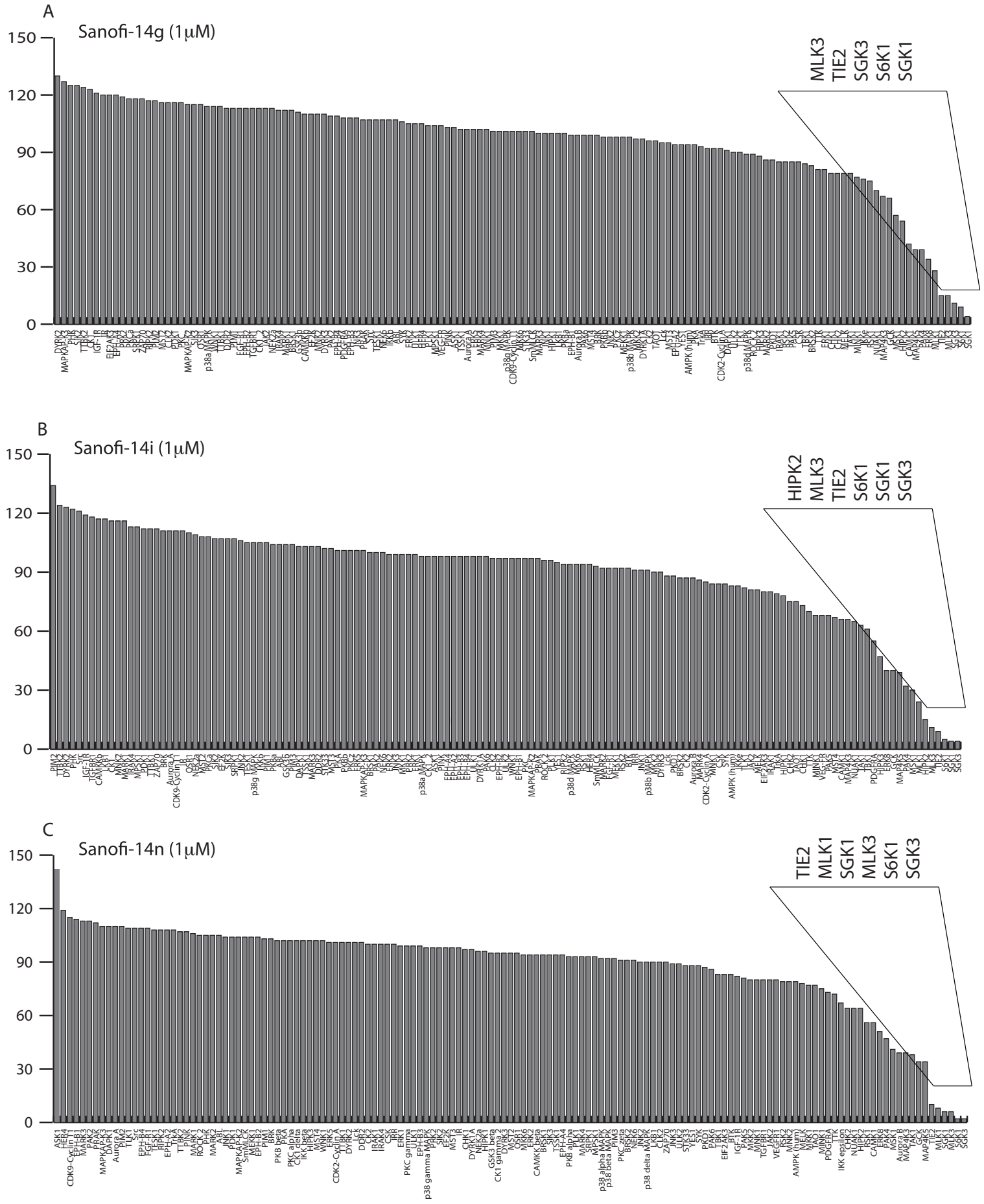

Supplementary Figure 5

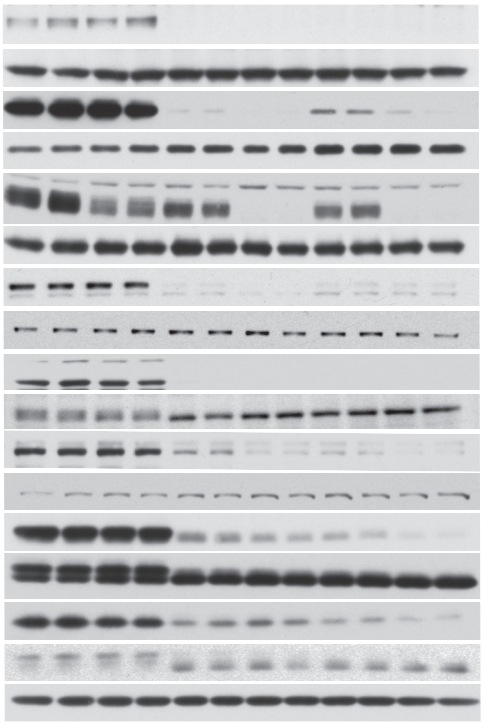

Supplementary Figure 6.

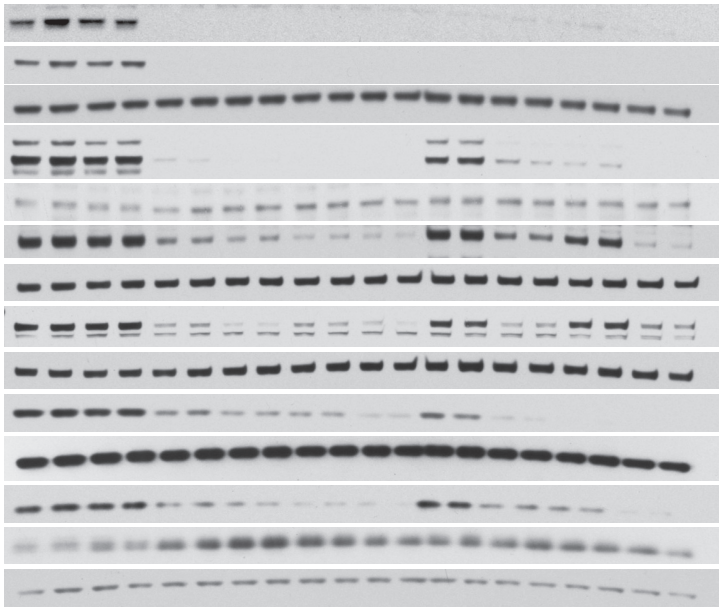

DMSO	+	-	-	-	-	-	-	-	-	-
VPS34-IN1, 1h	-	+	-	+	-	+	-	+	-	+
MK-2206, 1h	-	-	+	+	-	-	-	-	-	-
GDC0941, 1h	-	-	-	-	+	+	-	-	-	-
MK-2206, 5 days	-	-	-	-	-	-	+	+	-	-
GDC0941, 5 days	-	-	-	-	-	-	-	-	+	+

Supplementary Figure 7

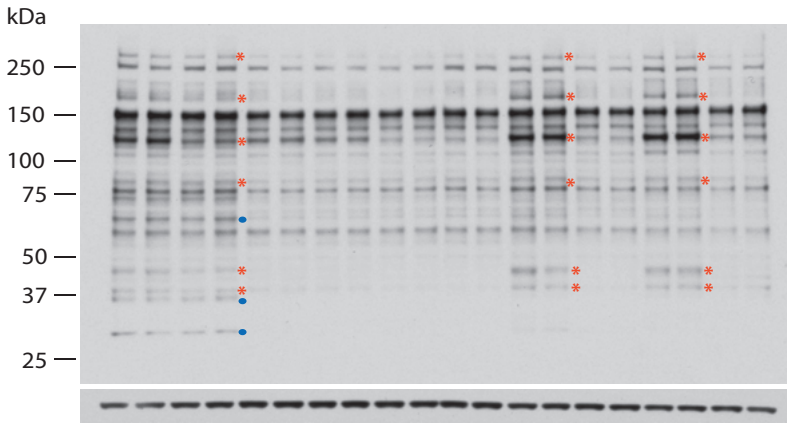

DMSO	+	-	-	-	-	-	-	-	-	-
14h, 1h	-	+	-	-	+	+	-	+	-	+
MK-2206, 1h	-	-	+	-	+	-	-	-	-	-
GDC0941, 1h	-	-	-	+	-	+	-	-	-	-
MK-2206, 5 days	-	-	-	-	-	-	+	+	-	-
GDC0941, 5 days	-	-	-	-	-	-	-	-	+	+

Supplementary Figure 8

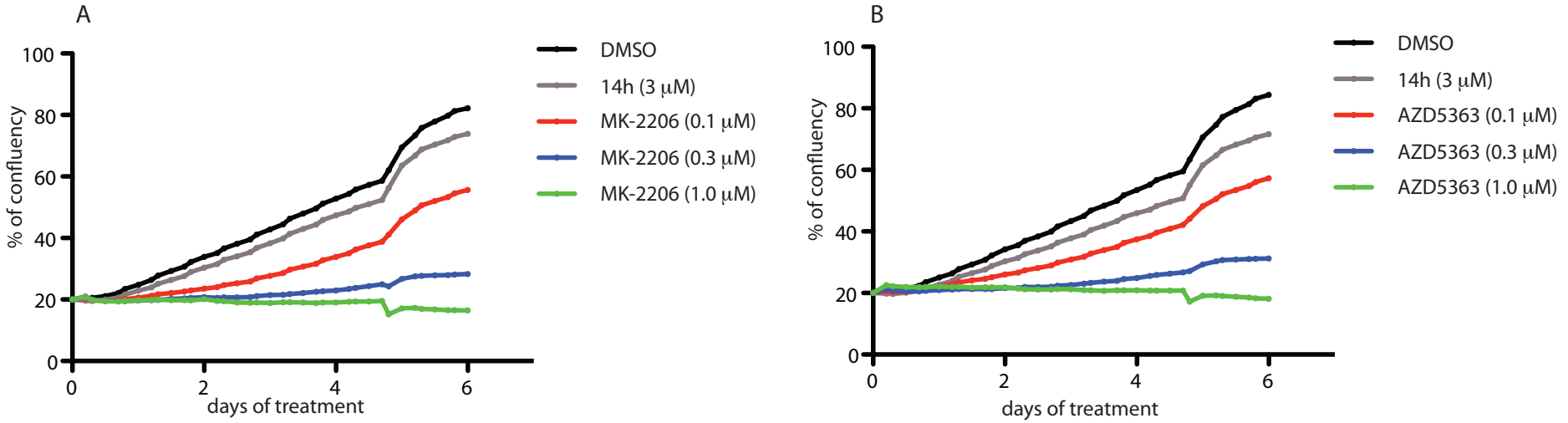

Supplementary Figure 9

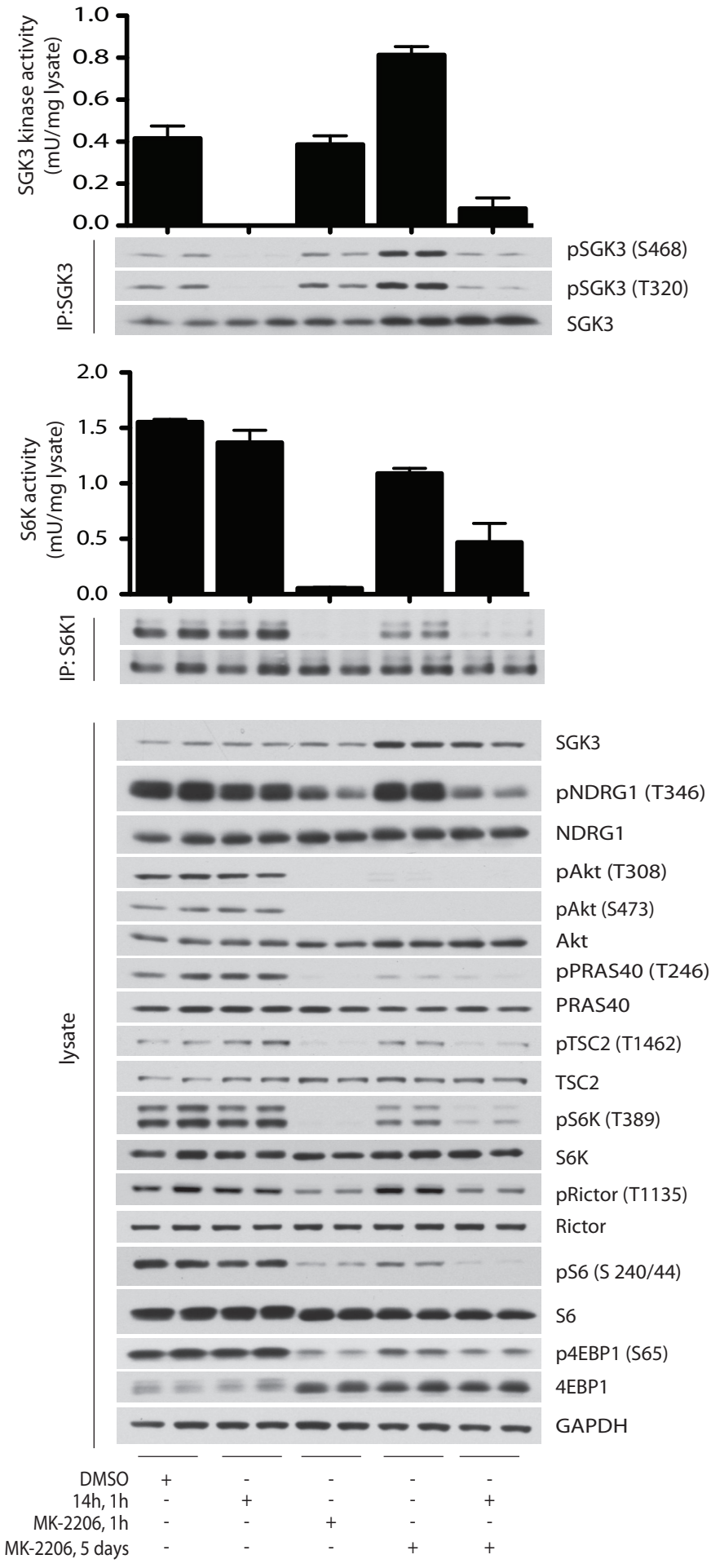

Supplementary Figure 10

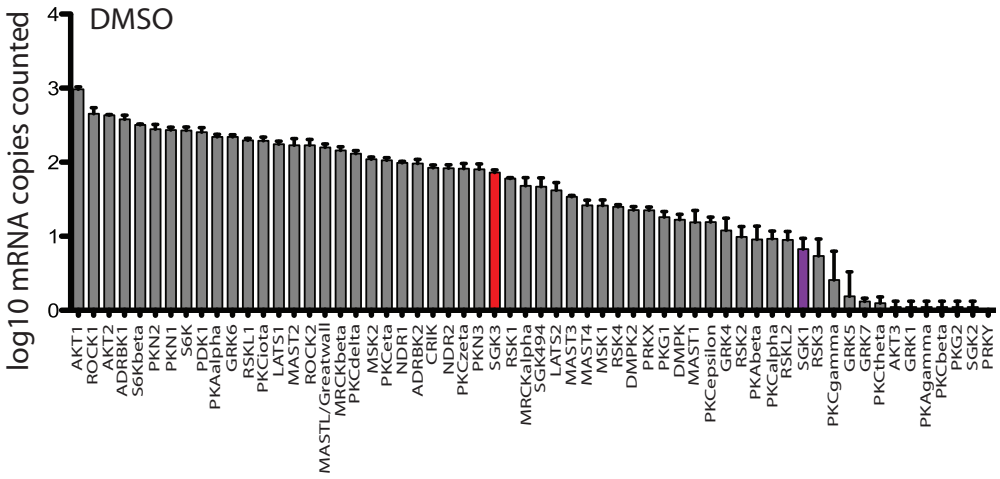

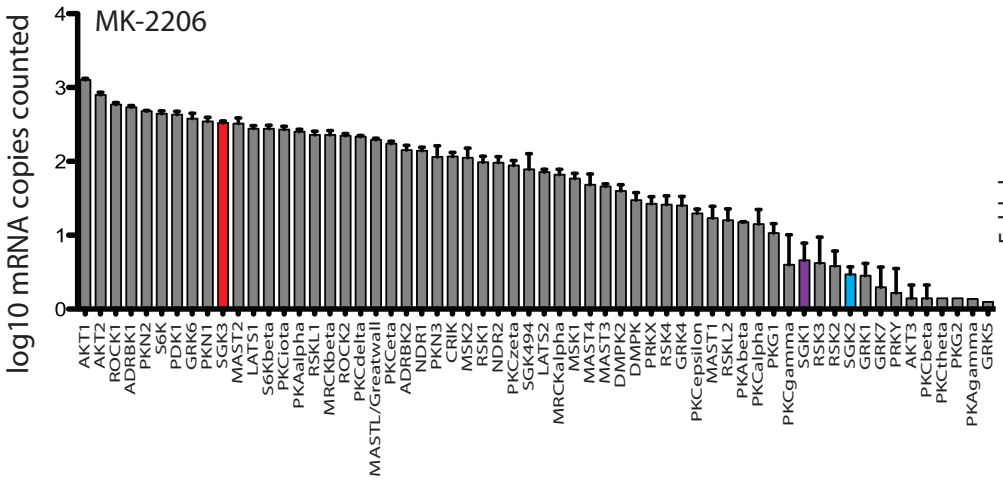

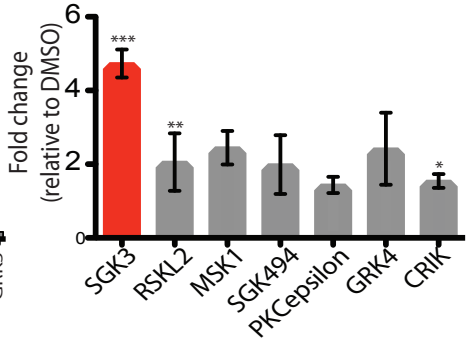

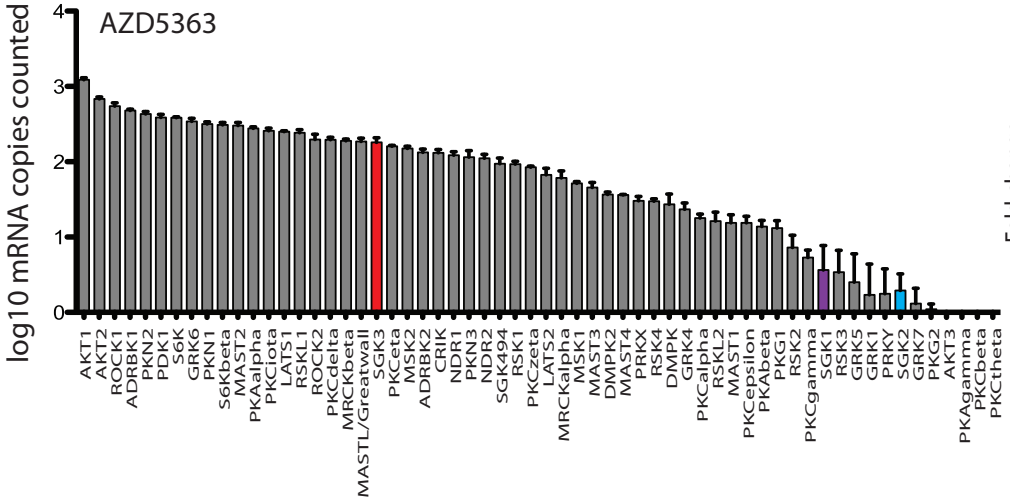

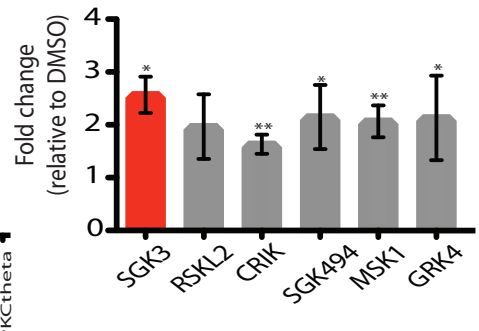

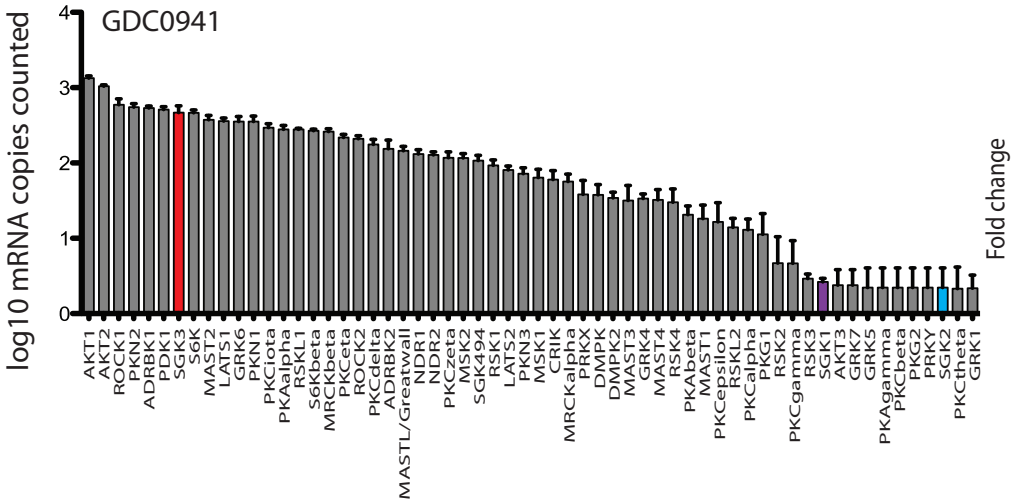

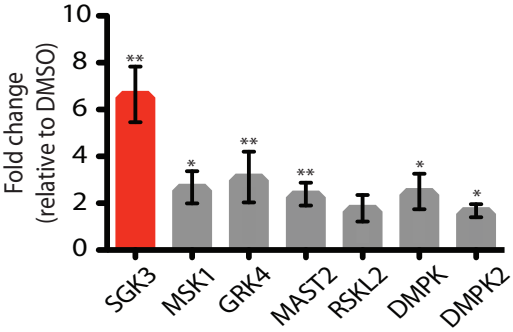

Supplementary Figure 11

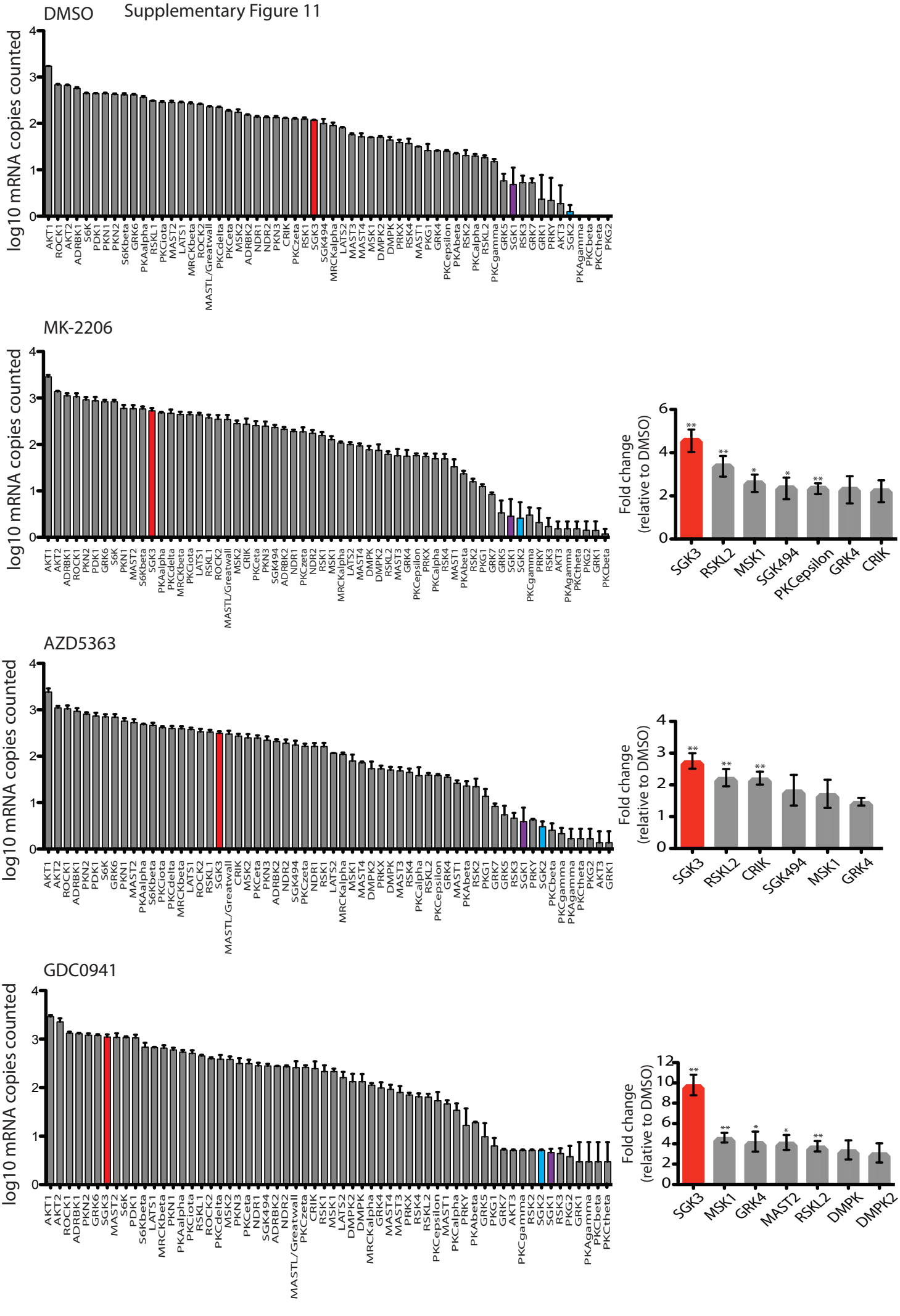

Supplementary TABLE 1. Sanofi-14g

kinase	% activity
DYRK2	130
MAPKAP-K3	127
PHK	125
SIK2	125
TTBK2	124
CK1 delta	123
IGF-1R	121
EIF2AK3	120
EPH-A4	120
IR	120
PRK2	119
PKC alpha	118
SRPK1	118
ZAP70	118
PIM2	117
RIPK2	117
PDK1	116
PKC gamma	116
CLK2	116
MST2	116
MAPKAP-K2	115
SIK3	115
OSR1	115
p38 alpha	114
TTBK1	114
WNK1	114
CK1 gamma	113
NEK2a	113
PIM1	113
TGFBR1	113
JAK2	113
EPH-B2	113
FGF-R1	113
DDR2	113
MARK1	112
BRSK1	112
IRAK4	112
GSK3 beta	111
MNK2	110
CAMKK beta	110
DYRK3	110
EF2K	110
PAK2	109
EPH-B4	109
JNK3	108
EPH-B3	108
PDGFRA	108

kinase	% activity
PRAK	107
NEK6	107
IKK beta	107
TESK1	107
Src	107
ABL	107
SYK	106
ERK2	105
ULK1	105
HER4	105
PLK1	104
MPSK1	104
VEGFR1	104
ASK1	103
PINK	103
ERK5	102
MNK1	102
Aurora A	102
MARK4	102
TSSK1	102
MKK1	101
MKK6	101
p38 gamma	101
STK33	101
SmMLCK	101
CDK9-Cyclin	101
PIM3	101
JNK1	100
PKB alpha	100
LKB1	100
MARK3	100
HIPK1	100
Aurora B	99
PAK6	99
MST4	99
BRK	99
EPH-B1	99
JNK2	98
p38 beta	98
PKB beta	98
PKC zeta	98
MEKK1	98
MKK2	97
DYRK1A	97
CK2	96
TAO1	96
MST3	95

kinase	% activity
Lck	95
PKA	94
AMPK	94
YES1	94
EPH-A2	94
TrkA	93
CDK2-Cyclin	92
BTK	92
IRR	92
DAPK1	91
TLK1	90
ULK2	90
p38 delta	89
ROCK 2	89
HIPK3	88
PKD1	86
MARK2	86
RSK2	85
PAK5	85
IRAK1	85
CSK	85
TBK1	84
BRSK2	83
ERK1	81
TTK	81
CHK1	79
CHK2	79
MELK	79
TAK1	79
MINK1	77
IKK epsilon	76
RSK1	75
NUAK1	70
MAP4K3	67
GCK	66
MSK1	57
HIPK2	54
CAMK1	42
PAK4	39
MAP4K5	39
ERK8	34
MLK1	28
MLK3	15
TIE2	15
SGK3	11
S6K1	9
SGK1	4

Supplementary TABLE 2. Sanofi-14h

kinase	% activity
MARK1	130
CSK	129
CK2	128
MAPKAP-K3	122
ASK1	121
ERK5	119
p38 alpha	117
ROCK 2	117
EPH-A2	117
Src	115
FGF-R1	115
p38 delta	114
MAPKAP-K2	114
MEKK1	114
MPSK1	114
CHK1	112
TLK1	112
PKC gamma	111
PIM1	111
TESK1	111
Lck	111
EPH-A4	111
TTBK2	110
PAK2	110
ZAP70	110
PKA	109
PHK	109
DYRK2	109
PLK1	108
SRPK1	108
IRAK4	108
PRAK	107
CDK9-Cyclin	107
PKC alpha	106
MARK4	106
PKB alpha	105
STK33	105
DAPK1	105
NEK6	105
IRR	105
DDR2	105
p38 gamma	104
MNK1	104
CDK2-Cyclin	104
BRSK1	104
MST4	104
NEK2a	103

kinase	% activity
WNK1	103
EPH-B2	103
HER4	103
JNK3	102
SIK3	102
PIM3	102
SmMLCK	101
SIK2	101
PAK6	101
SYK	101
TrkA	101
JNK2	100
CAMKK beta	100
Aurora A	100
CK1 delta	100
TTBK1	100
IKK beta	100
PIM2	100
ULK1	100
BRK	100
ERK2	99
TSSK1	99
MST2	99
OSR1	99
EPH-B3	99
EPH-B4	99
PINK	99
PKB beta	98
EF2K	98
HIPK3	98
EPH-B1	98
p38 beta	97
PKC zeta	97
MNK2	97
GSK3 beta	97
LKB1	97
BRSK2	97
IGF-1R	97
PDK1	96
AMPK	96
ERK1	95
MARK2	95
MARK3	95
RIPK2	95
YES1	95
JNK1	94
DYRK1A	94

kinase	% activity
DYRK3	94
TBK1	94
HIPK1	92
MKK6	91
MST3	91
CLK2	90
TAO1	90
IRAK1	90
ABL	90
PRK2	89
BTK	89
PDGFRA	89
PKD1	87
PAK5	87
ULK2	84
IR	82
CK1 gamma	81
EIF2AK3	81
TGFBR1	78
RSK2	77
TTK	77
JAK2	77
VEGFR1	73
MKK1	72
MINK1	71
MKK2	70
IKK epsilon	69
MELK	67
CAMK1	63
NUAK1	61
CHK2	50
RSK1	48
PAK4	46
HIPK2	45
TAK1	45
Aurora B	42
ERK8	38
GCK	34
MSK1	31
MAP4K3	25
MAP4K5	13
MLK1	10
TIE2	10
SGK1	6
MLK3	6
S6K1	3
SGK3	3

Supplementary TABLE 3. Sanofi-14i

kinase	% activity
PIM2	134
TTBK2	124
DYRK2	123
PHK	122
Src	121
IGF-1R	119
TGFBR1	118
CAMKK beta	117
LKB1	117
MNK2	116
MARK1	116
CK1 delta	116
IRAK4	113
MPSK1	113
PDK1	112
TTBK1	112
ZAP70	112
CDK9-Cyclin	111
Aurora A	111
BRK	111
IR	111
OSR1	110
NEK2a	109
PKC alpha	108
MST2	108
SIK2	107
SIK3	107
SRPK1	107
EF2K	107
JNK2	106
p38 gamma	105
IKK beta	105
PIM1	105
TESK1	105
PKB alpha	104
GSK3 beta	104
PIM3	104
ABL	104
DAPK1	103
MARK3	103
TSSK1	103
DDR2	103
STK33	102
MST3	102
ERK5	101
PKB beta	101
PKA	101

kinase	% activity
PKC zeta	101
MAPKAP-K3	101
BRSK1	100
NEK6	100
PAK2	100
MKK1	99
ERK1	99
ERK2	99
JNK3	99
PRK2	99
p38 alpha	98
CK1 gamma	98
DYRK1A	98
PAK6	98
ASK1	98
ULK1	98
EPH-A2	98
EPH-A4	98
EPH-B3	98
EPH-B4	98
PINK	98
PKC gamma	97
MAPKAP-K2	97
PRAK	97
CLK2	97
WNK1	97
ULK2	97
EPH-B1	97
EPH-B2	97
ROCK 2	96
PLK1	96
YES1	95
MKK6	94
p38 delta	94
RSK1	94
RIPK2	94
HER4	94
SmMLCK	93
RSK2	92
MARK2	92
MEKK1	92
BTK	92
FGF-R1	92
JNK1	91
p38 beta	91
IRR	91
MKK2	90

kinase	% activity
DYRK3	90
PKD1	88
Lck	88
Aurora B	87
BRSK2	87
CK2	87
MARK4	86
CDK2-Cyclin	85
MNK1	84
CSK	84
SYK	84
AMPK	83
IKK epsilon	83
TLK1	82
MELK	81
JAK2	81
EIF2AK3	80
IRAK1	80
TrkA	79
HIPK1	78
CHK2	75
TAO1	75
CHK1	73
TTK	70
PAK5	68
MINK1	68
VEGFR1	68
MST4	67
CAMK1	66
MAP4K3	66
NUAK1	65
TAK1	63
TBK1	61
PDGFRA	55
HIPK3	47
ERK8	40
GCK	40
MAP4K5	39
PAK4	32
MSK1	30
MLK1	24
HIPK2	15
MLK3	11
TIE2	9
S6K1	5
SGK1	4
SGK3	4

Supplementary TABLE 4. Sanofi-14n

kinase	% activity
ASK1	142
HER4	119
CDK9-Cyclin	115
EPH-B1	114
MARK3	113
PAK2	113
PRAK	112
MAPKAP-K3	110
DAPK1	110
Aurora A	110
PIM2	110
TLK1	109
Src	109
EPH-B4	109
FGF-R1	109
TESK1	108
RIPK2	108
EPH-A2	108
TrkA	108
TTBK2	107
PINK	107
MARK1	106
ROCK 2	105
PHK	105
MARK2	105
ABL	105
JNK1	104
PDK1	104
MAPKAP-K2	104
SmMLCK	104
MEKK1	104
EPH-B2	104
PIM1	103
BRK	103
PKB beta	102
PKA	102
PKC alpha	102
CK1 delta	102
IKK beta	102
HIPK3	102
MST4	102
WNK1	102
ERK5	101
CDK2-Cyclin	101
TTBK1	101
DYRK2	101
Lck	101

kinase	% activity
DDR2	101
CK2	100
IRAK1	100
IRAK4	100
CSK	100
IRR	100
ERK1	99
PKC gamma	99
ULK1	99
EPH-B3	99
p38 gamma	98
PRK2	98
SIK2	98
EF2K	98
MST3	98
IR	98
CHK1	97
DYRK1A	97
NEK2a	96
HIPK1	96
GSK3 beta	95
CK1 gamma	95
DYRK3	95
MST2	95
OSR1	95
MKK6	94
ERK2	94
CAMKK beta	94
BRSK1	94
SIK3	94
TSSK1	94
EPH-A4	94
PKB alpha	93
PLK1	93
MARK4	93
SRPK1	93
MPSK1	93
p38 alpha	92
p38 beta	92
PIM3	92
PKC zeta	91
BRSK2	91
NEK6	91
JNK2	90
p38 delta	90
LKB1	90
CLK2	90

kinase	% activity
ZAP70	90
JNK3	89
ULK2	89
STK33	88
YES1	88
SYK	88
PKD1	87
PAK6	86
TBK1	83
EIF2AK3	83
BTK	83
IGF-1R	82
PAK5	81
MKK2	80
MNK1	80
TGFBR1	80
JAK2	80
VEGFR1	80
RSK2	79
MNK2	79
AMPK	79
MELK	78
MKK1	77
TAO1	77
MINK1	75
PDGFRA	73
TTK	72
IKK epsilon	67
CHK2	64
NUAK1	64
HIPK2	64
RSK1	56
CAMK1	56
ERK8	51
PAK4	47
MSK1	41
Aurora B	39
MAP4K3	39
TAK1	38
GCK	34
MAP4K5	34
TIE2	10
MLK1	8
SGK1	6
MLK3	6
S6K1	2
SGK3	2